

SECURITY CLASSIFICATION OF THIS PAGE (When Data Entered)

REPORT DOCUMENTATION PAGE		READ INSTRUCTIONS BEFORE COMPLETING FORM
1. REPORT NUMBER AFFDL-TR-78-16	2. GOVT ACCESSION NO.	3. RECIPIENT'S CATALOG NUMBER
4. TITLE (and Subtitle)  WING PLANFORM GEOMETRY EFFECTS ON LARGE SUBSONIC MILITARY TRANSPORT AIRPLANES	5. TYPE OF REPORT & PERIOD COVERED Final Technical Report June 1977 - October 1977	
	6. PERFORMING ORG. REPORT NUMBER D6-46317	
7. AUTHOR(s)  Robert M. Kulfan and John D. Vachal	8. CONTRACT OR GRANT NUMBER(s)  F33615-76-C-3035	
9. PERFORMING ORGANIZATION NAME AND ADDRESS Boeing Commercial Airplane Company P.O. Box 3707 Seattle, Washington 98124	10. PROGRAM ELEMENT, PROJECT, TASK AREA & WORK UNIT NUMBERS Program Element Project 2404, Task 10 Work Unit 03	
11. CONTROLLING OFFICE NAME AND ADDRESS Air Force Flight Dynamics Laboratory/FXM Air Force Systems Command Wright-Patterson Air Force Base, Ohio 45433	12. REPORT DATE February 1978	
	13. NUMBER OF PAGES	
14. MONITORING AGENCY NAME & ADDRESS (if different from Controlling Office)	15. SECURITY CLASS. (of this report)  Unclassified	
	15a. DECLASSIFICATION/DOWNGRADING SCHEDULE	
16. DISTRIBUTION STATEMENT (of this Report)  Approved for public use, distribution unlimited.		
17. DISTRIBUTION STATEMENT (of the abstract entered in Block 20, if different from Report)		
18. SUPPLEMENTARY NOTES		
19. KEY WORDS (Continue on reverse side if necessary and identify by block number)  Military Transport Subsonic Transport Braced Wing		
20. ABSTRACT (Continue on reverse side if necessary and identify by block number)  A Preliminary Design Study of large turbulent flow military transport aircraft has been made. The study airplanes were designed to carry a heavy payload (350,000 lb) for a long range (10,000 nmi). The study tasks included:		

DD FORM 1473  
1 JAN 73

EDITION OF 1 NOV 65 IS OBSOLETE

SECURITY CLASSIFICATION OF THIS PAGE (When Data Entered)

## 20. Abstract (cont'd)

- . Wing geometry/cruise speed optimization of a large cantilever wing military transport airplane.
- . Preliminary design and performance evaluation of a strut-braced wing transport airplane.
- . Structural analyses of large-span cantilever and strut-braced wings of graphite/epoxy sandwich construction (1985 technology).

The best cantilever wing planform for minimum takeoff gross weight, and minimum fuel requirements as determined using statistical weight evaluations, has a high aspect ratio, low sweep, low thickness/chord ratio, and a cruise Mach number of 0.76. A near optimum wing planform with greater speed capability ( $M=0.78$ ) has an aspect ratio = 12, quarter chord sweep = 20 deg, and thickness/chord ratio of 0.14/0.08 (inboard/outboard).

Structural analyses were made of the large-span cantilever wing planforms. Using weight evaluations based on the structural analyses, it was determined that the gross weight of the near optimum configuration could be reduced by increasing the wing thickness/chord ratio to 0.15/0.10. The structural analyses indicated that the very large-span cantilever wings experienced significant deflections. Increasing wing thickness tended to alleviate deflection at taxi conditions, at the expense of increased fuel requirements.

Based on analytical (structural analyses) weights and projected improvements in strut/wing aerodynamic design, the strut-braced wing configuration was found to offer the potential of lower gross weight, lower empty weight, and reduced fuel consumption. The strut-braced wing configuration was effective in reducing the taxi deflections of very large-span wings.

Recommendations are given for additional studies necessary to determine design limitations, and performance and economic benefits of very large-span transport aircraft.

## **FOREWORD**

This is the final technical report on wing planform geometry effects on large subsonic military transport airplanes. This report, which has been assigned Boeing Document number D6-46317 for internal use, covers work performed by the Boeing Commercial Airplane Company, Seattle, Washington. This work was under the direction of Dr. Charles E. Jobe, Air Force Flight Dynamics Laboratory/FXM, Air Force Systems Command, Wright-Patterson Air Force Base, Ohio.

J. D. Vachal was the program manager and R. M. Kulfan was the technical integrator and principal investigator. Others supporting the effort were R. D. Anderson, V. D. Bess, W. N. Holmquist, K. Kumasaka, R. L. Sullivan, G. R. Swinford, J. H. Ward, H. Witonsky, and L. L. Wright.

# *Contrails*

**TABLE OF CONTENTS**

	Page
I. INTRODUCTION	1
II. STUDY APPROACH	3
III. CONFIGURATION DESCRIPTIONS	5
1. Reference Cantilever Wing Configuration, Model 767-768a	5
2. Strut-Braced Wing Configuration, Model 767-790a	9
3. Configuration Comparisons	12
IV. CONFIGURATION PERFORMANCE AND ECONOMICS	17
1. Mission Rules and Performance Objectives	17
2. Engine/Airframe Matching	18
3. Performance Comparisons	20
4. Life-Cycle Costs and Operating Costs Comparisons	25
V. CANTILEVER WING GEOMETRY/CRUISE SPEED OPTIMIZATION STUDY	29
1. Optimization Results	31
2. Cantilever Wing Configuration Selection	38
VI. LARGE-SPAN WING STRUCTURAL ANALYSES	41
1. Structural Sizing Criteria	41
2. Structural and Weight Analyses Methods	41
3. Cantilever Wing Structural Analyses	44
4. Strut-Braced Wing Structural Analyses	50
VII. RECOMMENDATIONS	55
VIII. CONCLUSIONS	57
REFERENCES	59

# *Contrails*

**LIST OF ILLUSTRATIONS**

Figure	Page
1. Study Technology Levels	3
2. Study Plan	6
3. Cantilever Wing Configuration, Model 767-768	7
4. Strut-Braced Wing Aerodynamic Considerations	10
5. Strut-Braced Wing Design Considerations	11
6. Strut-Braced Wing Configuration, Model 767-790	13
7. Cruise Drag Polar Comparison	16
8. Gross Weight Comparison	16
9. Flight Profile and Mission Rules	17
10. Cantilever Wing Airplane Engine/Airframe Matching	19
11. Cantilever Wing Airplane Design Selection	20
12. Strut-Braced Wing Airplane Engine/Airframe Matching	21
13. Strut-Braced Wing Design Selection	22
14. Large-Span Wing Comparisons	24
15. Twenty-year Life-cycle Cost Comparisons	25
16. Surge Condition Operating Cost Comparisons	27
17. Wing Parametric Optimization Study	30
18. Configuration Selections for the Aspect Ratio 8 Wing Designs	32
19. Configuration Selections for the Aspect Ratio 10 Wing Designs	32
20. Configuration Selections for the Aspect Ratio 12 Wing Designs	33
21. Configuration Selections for the Aspect Ratio 14 Wing Designs	33
22. Cruise Mach Number	34
23. Cruise Lift/Drag Ratio	34
24. Cruise Range Factor	35
25. Thrust/Weight Ratio	35
26. Block Fuel	36
27. Effect of Cruise Mach on Block Fuel	36
28. Takeoff Gross Weight	37
29. Cruise Mach Effect on TOGW	37
30. Productivity ( $M_{PL}/TOGW$ )	38
31. Structural Analysis Ground Rules	42
32. ORACLE – Structural Synthesis Program	43
33. Cantilever Wing Structural Analyses	45

## LIST OF ILLUSTRATIONS –(Cont'd)

Figure	Page
34. Cantilever Wing Equivalent Structural Material Thickness	46
35. Cantilever Wing Stiffnesses	47
36. Large-Span Wing Deflections	48
37. Wing Lift Distributions and Bending Moments	49
38. Comparison of Statistical and Analytical Weight Estimates – Cantilever Wings	50
39. Strut-Braced Wing Structural Analysis Methods	51
40. Strut-Braced Wing Structural Analyses	52
41. Strut-Braced Wing Equivalent Structural Material Thickness	53

## LIST OF TABLES

Table	Page
1. Initial and Updated Cantilever Wing Airplane Characteristics	8
2. Configuration Design Characteristics	14
3. Configuration Weight Comparison	15
4. Final Sized Airplane Characteristics, Model 767-768a and 767-790a	23
5. Airplane Sensitivities to Wing Weight Variations	24
6. Twenty-year Life-cycle Cost Elements, Based on Statistical Weights	26
7. Surge Condition Cost Elements, Based on Statistical Weights	27
8. Optimum Configurations and Design Sensitivities	39



## LIST OF ABBREVIATIONS AND SYMBOLS

A/C	Aircraft
AFFDL	Air Force Flight Dynamics Laboratory
All	Allowances
Alt	Altitude, ft
A/P	Airplane
AR	Aspect ratio = $b^2/s$
b	Span, ft
BL	Buttock line
BPR	Engine bypass ratio
C	Chord, constants, ft
$\bar{c}$	Mean aerodynamic chord
$C_D$	Drag coefficient = $D/q_s$
$C_{DF}$	Friction drag coefficient
$C_{DI}$	Induced drag coefficient = $C_L^2/\pi AR_e$
$C_{DM}$	Drag coefficient due to compressibility
$C_{DP}$	Profile drag coefficient
$C_F$	Flap chord
cg	Center of gravity
$C_L$	Lift coefficient = $L/q_s$
$C_{LR}$	Ratio of cruise $C_L$ to $C_L$ for maximum lift/drag ratio
Coeff	Coefficients
$c'$	Expanded flap due to Fowler action, ft
D	Drag
deg	Degrees
E	Modulus of elasticity, psi
f	Braced wing cutout thickness near the brace intersection, in.
$^{\circ}F$	Degrees Fahrenheit
$f_b$	Fuel burned, lb
$F_n$	Net thrust, lb
fpm	Feet per minute
ft	Feet
$fN( )$	Function of ( )

# Contrails

g	Acceleration due to gravity, ft/sec <sup>2</sup>
G	Shear modulus, psi
h	Height, ft
H/C	Honeycomb
I	Moment of inertia for wing bending, in. <sup>4</sup>
ICAC	Initial cruise altitude capability, ft
INBD	Inboard
J	Torsional constant, in. <sup>4</sup>
keas	Equivalent air speed, kts
ktas	True air speed, kts
kts	Knots
L	Lift, lb
lb	Pounds
L/D	Lift/drag ratio
LE	Leading edge
LFC	Laminar flow control
M	Mach number
MAC	Mean aerodynamic chord, ft
MAX	Maximum
mil	Military
MLA	Maneuver load alleviation
MODS	Modifications
MTW	Maximum taxi weight, lb
nmi	Nautical miles
n	vertical load factor
OEW	Operational empty weight, lb
OUTBD	Outboard
PL, P/L	Payload, lb
psi	Pounds per square inch
q	Dynamic pressure, psi = $\frac{1}{2}\rho V^2$
R	Range, nmi
ref	Reference
REPL	Replacement
S	Wing area, ft <sup>2</sup>
SE	Spare engines

# Contrails

sec	Seconds
SFC	Specific fuel consumption
SLST	Sea level static thrust
SOB	Side of body
SP	Spares
STA	Station
S <sub>W</sub>	Wing area
t	Thickness, in.
$\bar{T}$	Equivalent structural material thickness, in.
t/c	Thickness/chord ratio
TE	Trailing edge
TOGW	Takeoff gross weight, lb
T/W	Thrust/weight ratio
V	Velocity, ft/sec
V <sub>APP</sub>	Approach velocity, ft/sec
V <sub>B</sub>	Design speed for maximum gust intensity
V <sub>C</sub>	Design cruising speed
V <sub>D</sub>	Design dive speed
V <sub>E</sub>	Equivalent air speed
Vol	Volume, ft <sup>3</sup>
V <sub>S</sub>	Stall speed, ft/sec
W/b <sup>2</sup>	Span loading, lb/ft <sup>2</sup>
WL	Waterline
W/S	Wing loading, lb/ft <sup>2</sup>

## SYMBOLS

$\Delta$	Incremental amount
$\eta$	Semispan fraction
$\lambda$	Taper ratio
$\Lambda$	Sweep angle
$\pi$	Pi=3.1416; empennage arrangement
$\rho$	Density

# *Contrails*

## SUBSCRIPTS

app	Approach
C/4	Quarter chord
F	Flap
Max	Maximum
OPT	Optimum
St	Strut

## SECTION I

### INTRODUCTION

Increased concern about the cost and availability of aviation fuel, in addition to possible requirements for global-range movement of large payloads, suggests a need for efficient military transport aircraft designs that conserve fuel.

The recently completed AFFDL/Boeing Boundary Layer Control Technology Application study<sup>(1)</sup> evaluated large military transport designs that incorporated various advanced aerodynamic concepts. The study identified laminar flow control (LFC) as the aerodynamic concept offering the greatest potential for conserving fuel. A more in-depth preliminary design study<sup>(2)</sup> was then conducted to further assess the potential performance and economic benefits of the application of LFC to very large military transport airplanes. These later results indicated that LFC can provide large reduction in fuel usage, and lower gross weights. The life-cycle costs were found to be very dependent on airplane utilization, on technology complexity costs, and on LFC total systems weight.

Purpose of the study reported herein was to conduct a preliminary design investigation of a large turbulent flow military transport airplane. Study tasks included:

- Wing geometry/cruise speed optimization of a large turbulent flow cantilever wing military transport airplane
- Preliminary design and performance evaluation of a strut-braced wing transport airplane
- Performance and economic comparisons between the strut-braced wing and cantilever wing configurations
- Aeroelastic structural analyses of very large-span wings of graphite/epoxy sandwich construction (1985 technology)

The study approach is described in Section II. Final configuration characteristics, performance, and economic comparisons are presented in Sections III and IV. Section V describes the cantilever wing geometry/cruise speed optimization study. Structural analyses of the large-span wings are summarized in Section VI. The remaining sections contain research and development recommendations, and the main study conclusions.

1. Kulfan, R. M., and Howard, W. M.: "Application of Advanced Aerodynamic Concepts to Large Subsonic Transport Airplanes," Tech. Report AFFDL-TR-75-112, November 1975.
2. Kulfan, R. M., and Vachal, J. D.: "Application of Laminar Flow Control to Large Subsonic Military Transport Airplanes," Tech. Report AFFDL-TR-77-65, July 1977.

# *Contrails*

## SECTION II STUDY APPROACH

Design mission objectives for the study configurations included:

- Range = 10,000 nmi
- Payload = 350,000 lb
- Takeoff field length = 9,000 ft
- Mach number: determined by tradeoff studies

Payload density limits were set by the requirements to carry either 75 military standard cargo containers or three M-60 tanks.

The general technology level assumed for the study configurations, as shown in Figure 1, corresponds to projections that would allow start of prototype production in 1985. First flight would occur in 1988 or 1989, and airplane in service would be after 1990.

This study used the substantial data base of Boeing in-house large freighter studies, and of the previously mentioned USAF/Boeing advanced aerodynamic technology studies, to provide design ground rules and configuration development guidance.

The design development and analyses methods that were used to develop each of the study configurations are described in Reference 2.

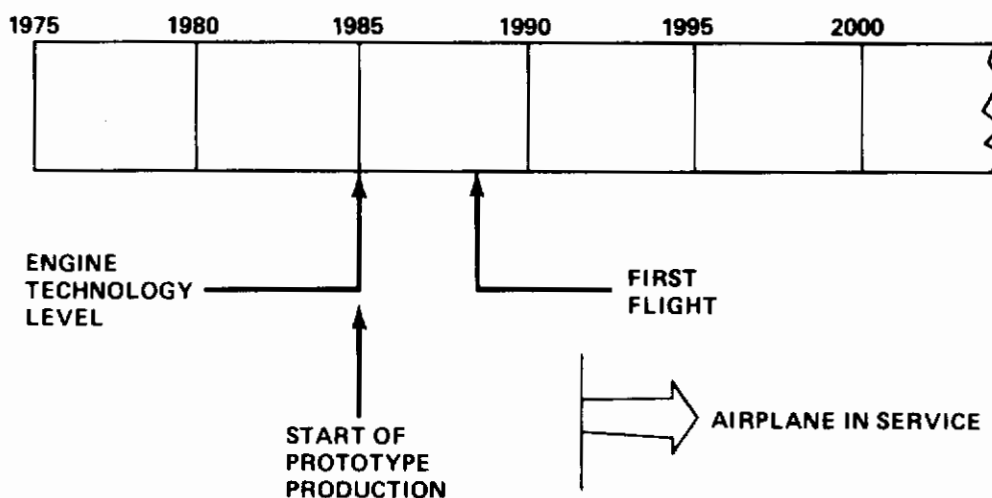


Figure 1 Study Technology Levels

# Contrails

The approach used to achieve study objectives is summarized in Figure 2. The initial task was to define the reference cantilever airplane configuration. This configuration was derived from the reference turbulent airplane, Model 767-768, of Reference 2.

A wing geometry/cruise speed parametric optimization study was then conducted for this cantilever wing configuration. Results of the parametric optimization study substantiated the selection of wing planform characteristics of the new reference configuration Model 767-768a.

A baseline strut-braced wing configuration was developed from the reference cantilever wing configuration, with structural and aerodynamic design guidelines from Boeing in-house braced-wing large freighter studies. The strut arrangement selection was guided by specifically conducted structural analyses. The baseline strut-braced wing configuration was then sized to meet the mission objectives. The sized strut-braced wing configuration Model 767-790a definition was then completed.

Economic analyses were then made of the cantilever wing configuration, Model 767-768a, and the strut-braced wing configuration, Model 767-790a. Calculations were made of 20-year life-cycle costs, and of 60-day surge condition operating costs.

The aforementioned design, parametric, and economic analyses incorporated statistically derived parametric weight evaluations.

Detailed analytical structural and weight analyses were then conducted for the final cantilever wing and braced-wing configurations. Additional structural and weight analyses were made for the cantilever wing, with increased wing thickness distributions. Results of these detailed weight evaluations were combined with the weight sensitivity study results to finalize the cantilever wing configuration and braced-wing configuration performance comparisons.

Characteristics of the final cantilever wing and braced-wing configurations are discussed in Section III.



## SECTION III

### CONFIGURATION DESCRIPTIONS

This section contains a description of the final cantilever wing and strut-braced wing configurations. Considerations that led to the final configuration arrangements are discussed below. The performance and economic evaluations of the final configurations are discussed in Section IV.

#### 1. REFERENCE CANTILEVER WING CONFIGURATION, MODEL 767-768a

The reference cantilever wing configuration for the study reported herein was derived from the baseline turbulent flow configuration, Model 767-768 of Reference 2, which is shown in Figure 3. Model 767-768 was reanalyzed, and the following updates were made: a 3% reduction in reserve fuel allowances, a 3% increase in induced drag for nonoptimum span loading, and an increase in the takeoff field length calculation temperature to 90°F, instead of the original 59° F. Model 767-768 was resized with these updated inputs to define the present reference cantilever configuration, Model 767-768a. Fuel requirements and gross weight increased by approximately 2% as a result of these updates. The weight and geometrical characteristics of Model 767-768, and the updated configuration Model 767-768a, are shown in Table 1.

Geometrical features of Model 767-768a are illustrated in Figure 3. The reference configuration features a three-bay oval fuselage that was dictated by design payload requirements. This arrangement provides the necessary space for the low-density payload of 75 military cargo containers without requiring excessive cargo floor length. The kneeling landing gear results in a cargo floor loading height of 84 in. The body has front and aft loading capability for the cargo containers and for light vehicles. The high-density payload consisting of three M-60 tanks requires front loading and unloading. The fuselage has an advanced one-piece windshield design to minimize forebody drag. This design provides direct viewing, and incorporates a conventional flight deck with state-of-the-art displays and controls for the 1985 time period. The design would require development of an optically corrected smooth structural windshield and a seamless seal assembly.

Wing planform characteristics were selected for efficient long-range cruise considerations incorporating the benefits of active controls and advanced composites structural materials. The high-lift system includes 747 SP-type single-slotted trailing-edge (TE) flaps, and variable camber leading-edge (LE) flaps. The TE flap has a chord ratio ( $C_F/C$ ) of 0.225 and a Fowler motion ( $C^1/C$ ) of 1.08.

The canted "π" tail empennage arrangement is a structurally efficient design that provides the desired drive-through and air-drop capability. The use of active controls, together with the double-hinged rudder, results in minimum tail areas.

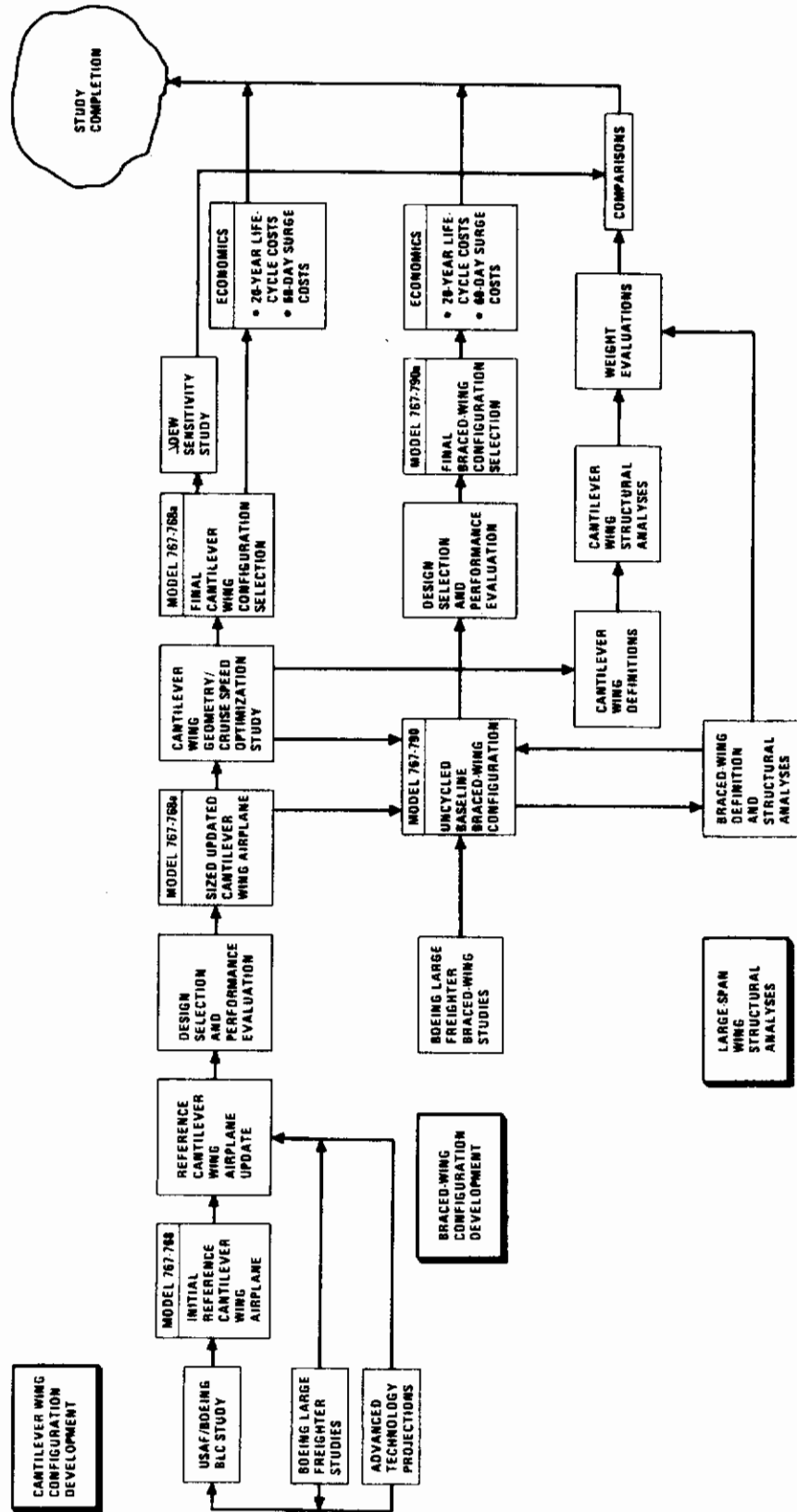


Figure 2 Study Plan

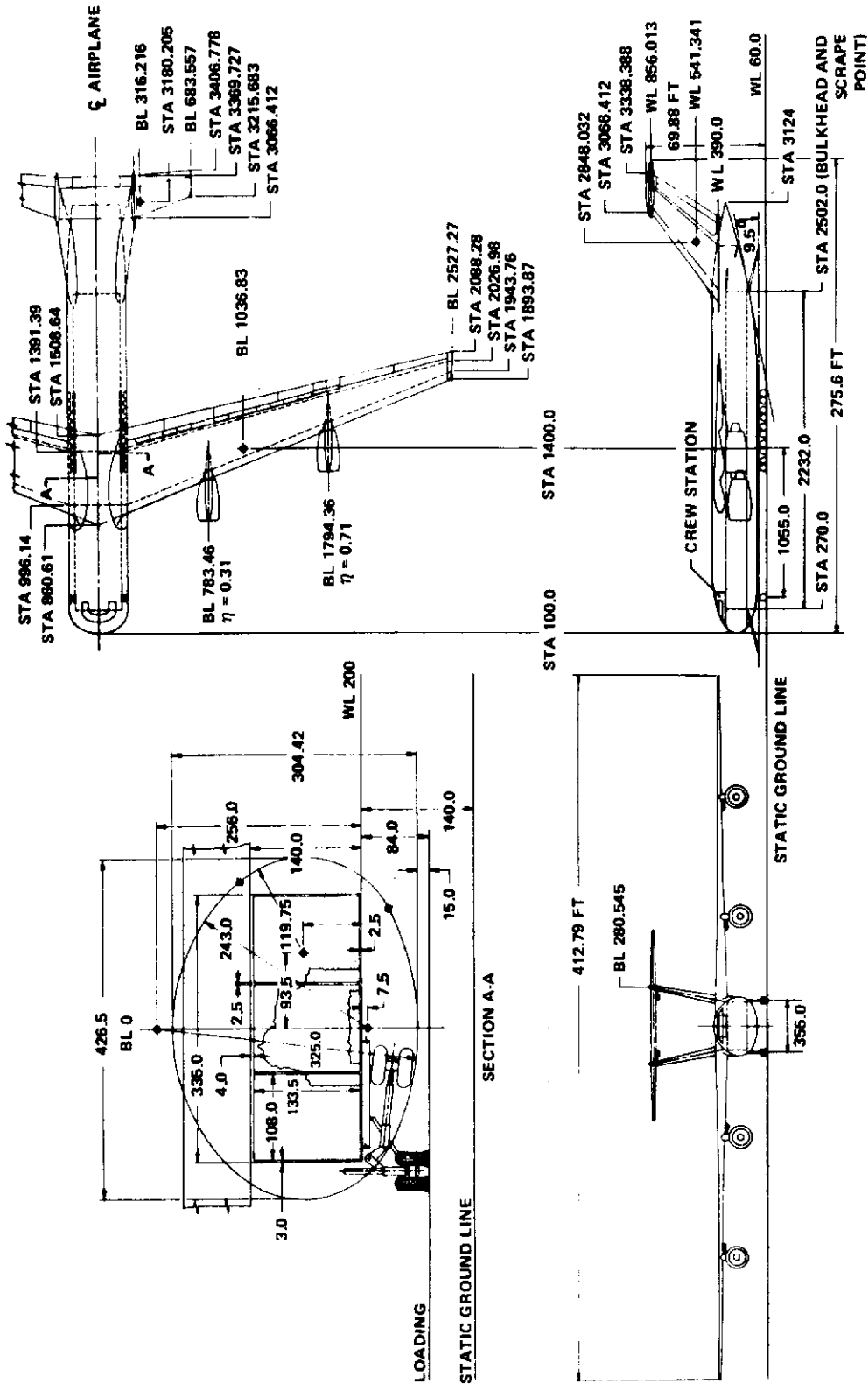
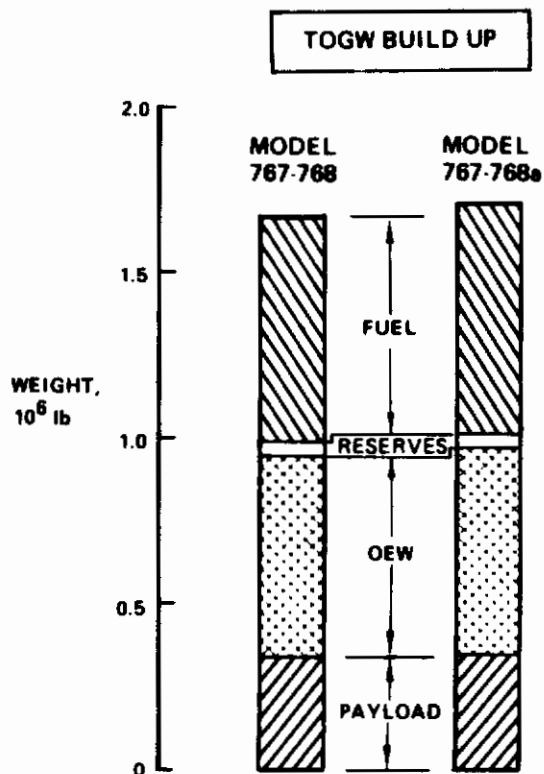


Figure 3 Cantilever Wing Configuration, Model 767-768

**Table 1 Initial and Updated Cantilever Wing Airplane Characteristics**

ITEM		INITIAL CANTILEVER WING AIRPLANE, MODEL 767-768	UPDATED CANTILEVER WING AIRPLANE, MODEL 767-768a
Design mission	Payload, lb Range, nmi	350,000 10,000	
Weights, lb	TOGW OEW Block fuel Reserves	1,665,800 608,600 668,600 43,300	1,701,560 628,230 685,050 42,880
Wing	Area, ft <sup>2</sup> AR t/c Inboard/outboard $\Lambda_{c/4}$ , deg W/S, lb/ft <sup>2</sup>	14,785 12 0.14/0.08 20 112.7	15,755 12 0.14/0.08 20 108.0
Engine	Engine type/no./BPR	STF 482/4/7.5	
	SLST, lb T/W, lb/lb	77,200 0.185	80,720 0.190



The propulsion system includes four 1985 technology high bypass ratio (BPR) engines. The engines are located on the wing primarily because of airplane balance requirements and engine design constraints (SLST $\leq$ 90,000 lb) that require a minimum of four engines for the study airplanes. Airplane balance is the correct relationship of the center of gravity (cg) of the airplane to aerodynamic stability limits for different loading conditions. This relationship is more difficult to achieve when the engines are on the aft fuselage, especially for aircraft with heavy payloads and large high bypass ratio engines. Because of the difference between the position of the payload cg and the propulsion system cg, large shifts in the airplane cg would occur from one operating condition to the next. The spanwise locations were set by flutter considerations and provide wing bending relief.

## 2. STRUT-BRACED WING CONFIGURATION, MODEL 767-790a

A strut-braced wing offers the possibility of structurally efficient large-span wings. Consequently, a strut-braced wing configuration was developed from the reference cantilever wing configuration to explore the potential performance, economics, and structural benefits.

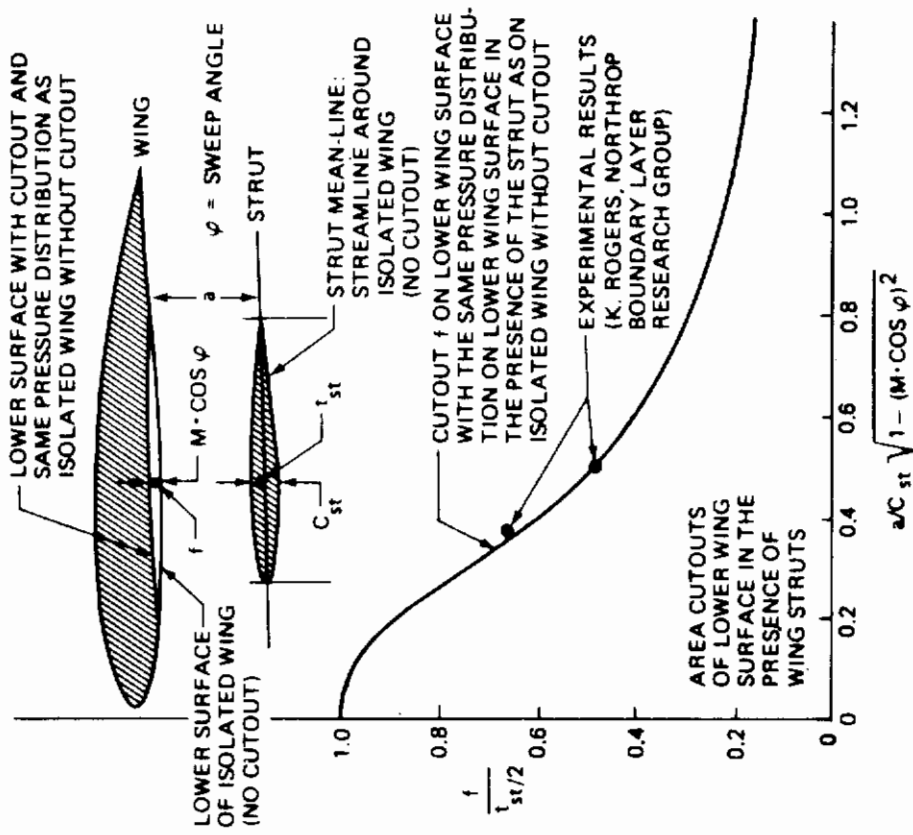
Results of Boeing in-house strut-braced wing large freighter studies were used to provide aerodynamic and structural design guidance in defining the wing/strut arrangement. The success of a strut-braced wing is very dependent on achieving a structurally efficient design without encountering significant wing/strut unfavorable interference effects. Previous Northrop studies and recent Boeing wind tunnel results (Figure 4) indicate that aerodynamic interference between wing and strut can be minimized by proper tailoring of the wing and/or strut, particularly near the wing/strut intersection. Additional detailed aerodynamic design and test verification are necessary to identify minimum strut effects on profile and on compressibility drag. An interference factor of 10% was applied to the strut-isolated profile drag, and a critical Mach decrement of 0.01 was used to account for strut interference effects in the study reported herein.

A large number of design variables must be examined to fully optimize a strut-braced wing design. Consequently, results of aforementioned Boeing strut-braced wing studies, such as shown in Figure 5, were used to define the strut-braced wing configuration for this study. Design guidelines used to develop the strut-braced wing configuration included:

- Strut/wing attachment angle = 12 deg
- Strut thickness/chord ratio = 10%. This is 2% greater than the outboard wing thickness.
- The wing planform outboard of the attachment station is geometrically similar to the reference cantilever wing planform (Model 767-768a).
- Inboard of the strut attachment station, the wing chord is held constant.
- The sweep of the strut and the wing quarter chord sweep are equal (20 deg).

B. STRUT CAMBER EFFECTS

A. WING CONTOUR EFFECTS



REF: W. PFENNINGER; "SOME THOUGHTS ON THE DESIGN OF LARGE GLOBAL RANGE LFC TRANSPORT AIRPLANE"

WING  
AR = 15  
 $\Lambda_{c/4} = 31^\circ$   
 $\eta_{STRUT} = 0.60$

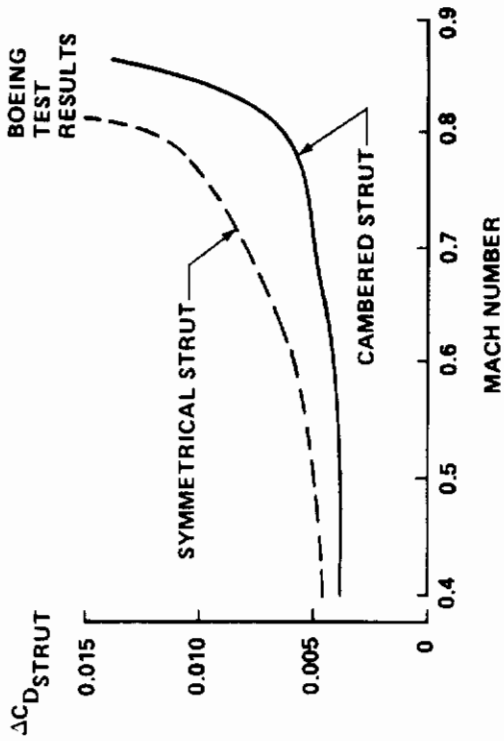
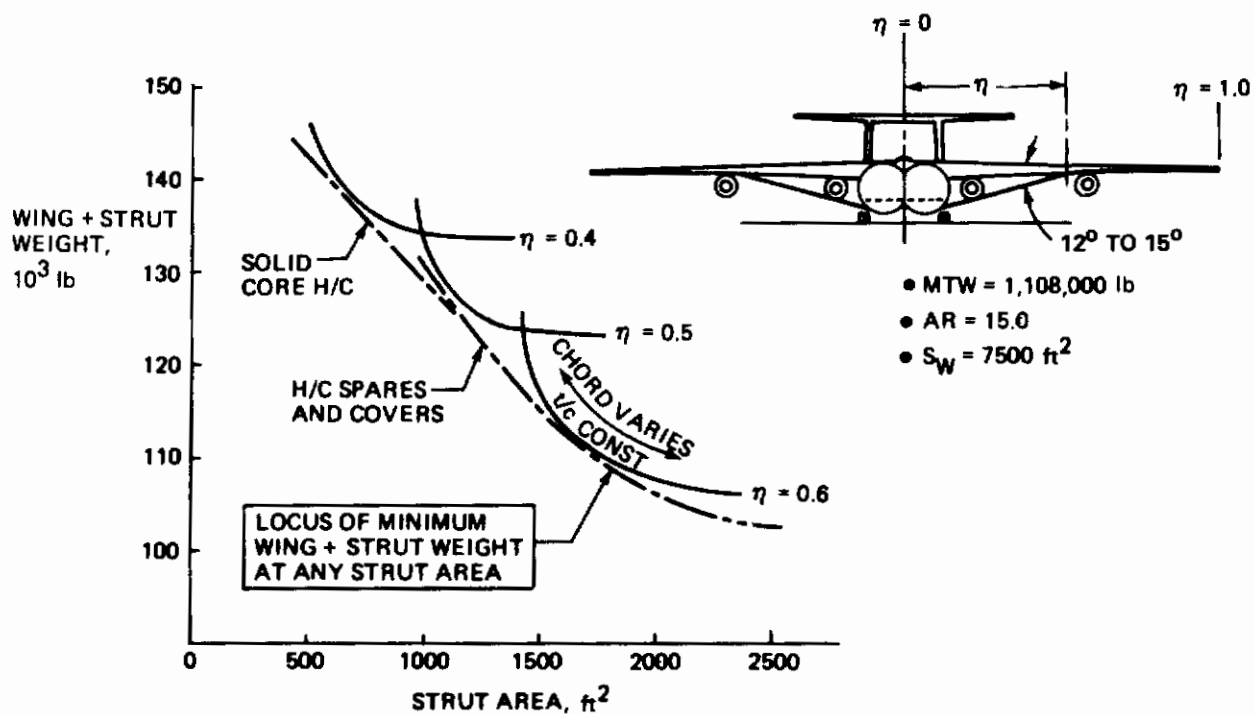


Figure 4 Strut-Braced Wing Aerodynamic Considerations



## ● STRUT ATTACHMENT



- (A) WING PLANFORM OUTBOARD OF STRUT SAME AS CANTILEVER WING PLANFORM
- (B) CONSTANT CHORD INBOARD WING
- (C) WING SWEEP:  $\Delta c/4 = 20^\circ$
- (D) MAIN STRUT CHORD = 50% WING CHORD
- (E) MAIN STRUT SWEEP =  $20^\circ$ ,  $t/c = 10\%$
- (F) JURY STRUT AT MAIN STRUT MIDSPAN,  $t/c = 5\%$
- (G) JURY STRUT CHORD = 50% MAIN STRUT

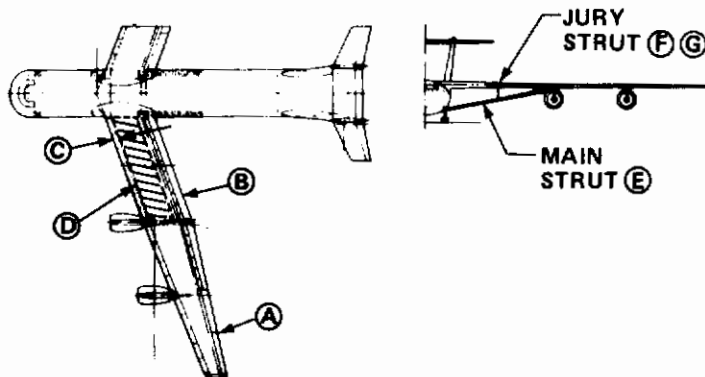


Figure 5 Strut-Braced Wing Design Considerations

The chord of the strut was determined as the maximum chord length that satisfies the following criteria:

- 1) Strut sweep equals wing sweep.
- 2) Leading edge of the strut falls behind the leading-edge flaps at the outboard attachment station.
- 3) Strut attaches to the fuselage bulkhead ahead of the foremost main landing gear.

These criteria resulted in a strut chord equal to one-half the wing chord.

The wing thickness/chord definition is the same as on the reference cantilever wing (14% inboard, 8% outboard). The braced wing is thinner inboard than the reference wing because of the reduced inboard wing chords. The braced wing was "sheared-up" inboard equal to half the reduction in wing thickness, so that the top of the wing matches the reference configuration at the wing body junction. This provides the greatest wing/strut spacing at the body without changing the fuselage design. The combination of strut attachment angle and side of the body wing/strut spacing results in a strut attachment of approximately 45% wing semispan.

The inboard engine is located at the strut attachment station. The engine/strut/wing attachment provides a minimum wing/strut separation distance of 20 in. The outboard engine location is unchanged relative to the cantilever wing location. The leading-edge and trailing-edge flaps, spoilers, etc., are constant length inboard of the strut attachment station.

The shortened inboard wing chords reduced the wing area. Consequently, the aspect ratio was increased from 12 to approximately 13.5.

Initial structural analyses of the strut-braced wing indicated the desirability of a jury strut. Consequently, the final strut-braced wing definition includes a 5% thick jury strut located at midspan of the main strut. The jury strut chord is one-half of the main strut chord. The strut-braced wing design considerations are summarized in Figure 5.

The general arrangement of the strut-braced wing configuration that was developed from the aforementioned design guidelines is shown in Figure 6.

### 3. CONFIGURATION COMPARISONS

Geometrical characteristics of the final sized cantilever wing and strut-braced wing configurations are summarized in Table 2. Group weight statements are shown in Table 3. Cruise drag comparisons are shown in Figure 7. The cantilever wing and strut-braced wing configurations have relatively high lift/drag ratios (27.8 and 26.7, respectively). This is because of the large wing span/wetted area ratio.

Gross weight comparisons of the study configurations are shown in Figure 8. Initial comparisons based on parametric statistical weights indicate that the gross weight of the cantilever wing configuration is slightly less than that of the strut-braced wing. Airplane evaluations using analytical weights, based on the detailed structural analyses (described in Section VI), indicate that the strut-braced wing configuration has approximately 4% less gross weight than the cantilever wing configuration.



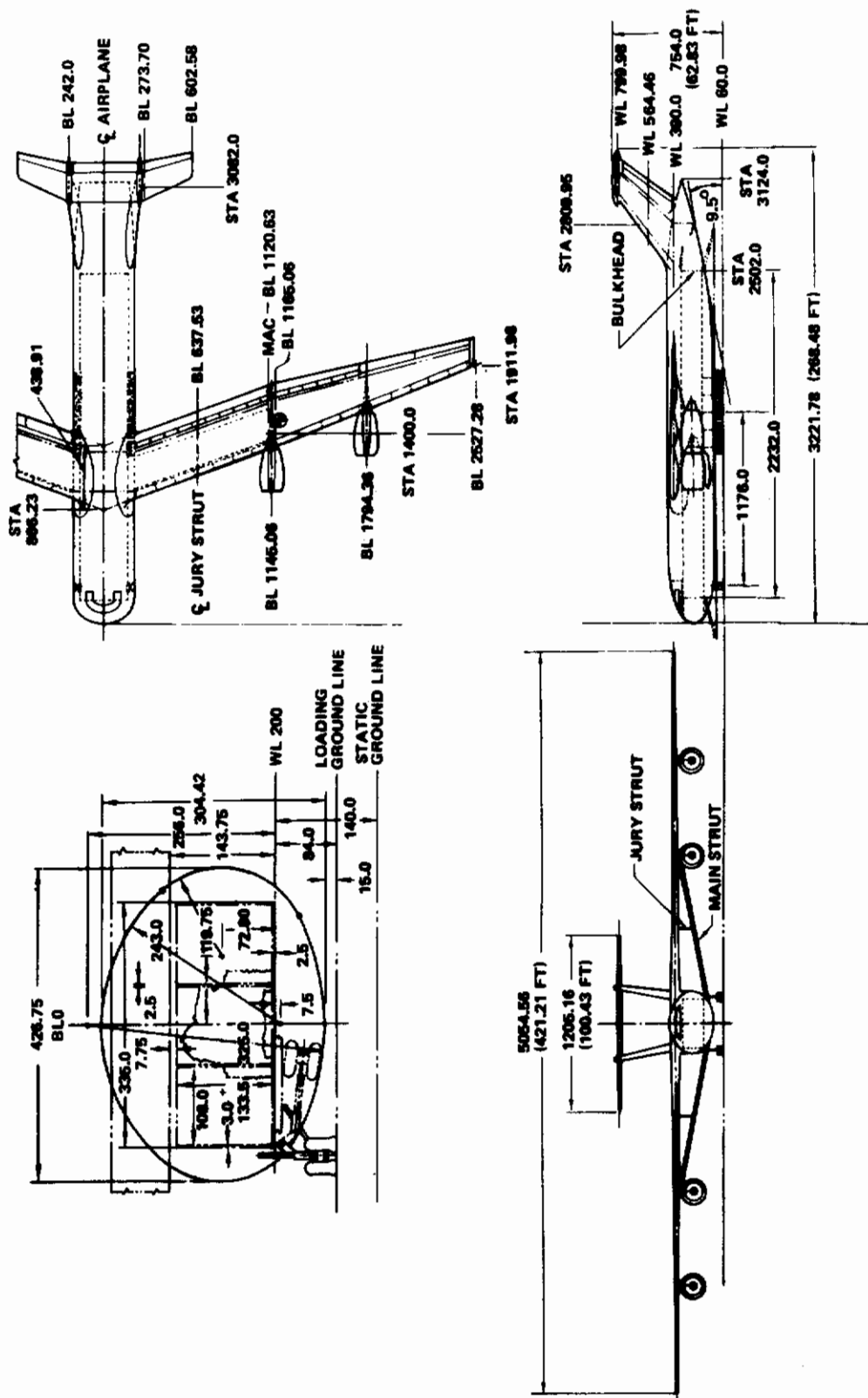


Figure 6 Strut-Braced Wing Configuration, Model 767-790

Table 2 Configuration Design Characteristics

		CANTILEVER WING AIRPLANE, MODEL 767-768a	STRUT-BRACED WING AIRPLANE, MODEL 767-790a
<b>MAJOR DESIGN PARAMETERS</b>	Payload, lb	350,000	
	Range, nmi	10,000	
	Cruise Mach number	0.78	0.77
	Mil TOFL, ft	9,000	
Weights	TOGW, lb	1,701,560	1,734,250
	OEW, lb	628,230	623,680
	Fuel, lb	685,050	721,620
	Reserves, lb	42,880	44,020
Fuselage	Length, lb	252	
	Max diameter, in.	426.5	
	Wetted area, ft <sup>2</sup>	21,927	
Landing gear	Nose	4(49 x 17)	
	Main	40(49 x 17)	
Wing	Area, ft <sup>2</sup>	15,755	14,450
	Wetted area, ft <sup>2</sup>	27,676	26,143
	AR	12	13.4
	$\Lambda_c/4$ , deg	20	
	Span, ft	434.8	440.0
	$\lambda$ , inboard/outboard	0.30	0.0/0.63
	MAC, ft	39.7	35.8
	t/c, root/tip	0.14/0.08	
Horizontal tail	Area, ft <sup>2</sup>	2,628	2,375
	Wetted area, ft <sup>2</sup>	5,250	4,744
	AR	5.07	
	$\Lambda_c/4$ , deg inboard/outboard	0.0/22.5	
	$\lambda$ , inboard/outboard	0.0/0.63	
	t/c	0.11	
	MAC, ft	23.2	22.1
	Tail vol coeff	0.615	0.669
Vertical tail	Area, ft <sup>2</sup>	2,624	2,467
	Wetted area, ft <sup>2</sup>	5,248	4,934
	AR	1.0	
	$\Lambda_c/4$ , deg	54	
	$\lambda$	0.52	
	t/c	0.12	
	MAC, ft	40.0	38.8
	Tail vol coeff	0.044	0.045
Propulsion	Type/BPR	STF 482/7.5	
	Number/Location	4/wing mounted	
	SLST, lb	80,720	81,770
	Wetted area, ft <sup>2</sup>	3,261	3,304

**Table 3 Configuration Weight Comparison**

ITEM	CANTILEVER WING CONFIGURATION, MODEL 767-768, lb	CANTILEVER WING CONFIGURATION, MODEL 767-768a, lb	BRACED WING CONFIGURATION, MODEL 767-790a, lb
Wing	211,000	223,170	217,570
Horizontal tail	11,900	12,300	11,120
Vertical tail	15,430	16,920	15,910
Body	186,630	187,460	187,820
Main gear	37,600	37,940	38,380
Nose gear	5,760	6,180	6,250
Nacelle and strut	23,800	24,900	25,220
<b>Total structure</b>	<b>492,210</b>	<b>508,870</b>	<b>502,270</b>
Engine	50,030	52,710	53,520
Engine accessories	1,330	1,330	1,330
Fuel system	6,740	7,040	6,640
Engine controls	320	320	320
Starting system	320	320	320
Thrust reverser	6,770	7,090	7,180
<b>Total propulsion group</b>	<b>65,615</b>	<b>68,810</b>	<b>69,310</b>
Auxiliary power unit	2,000	2,000	2,000
Instruments and nav equipment	1,270	1,270	1,270
Surface controls	21,310	21,290	22,360
Hydraulic/pneumatic	4,680	4,770	4,860
Electrical	3,120	3,120	3,120
Avionics	3,140	3,140	3,140
Furnishings and equipment	6,710	6,710	6,710
Air conditioning and equipment	3,620	3,620	3,620
Auxiliary gear	270	270	270
<b>Total fixed equipment</b>	<b>46,120</b>	<b>46,190</b>	<b>47,350</b>
Manufacturer's empty weight	603,840	623,870	618,930
Crew	1,290	1,290	1,290
Crew provisions	320	320	320
Oil and trapped oil	600	600	600
Unavailable fuel	800	800	800
Payload provisions	1,750	1,750	1,750
<b>Total nonexpended useful load</b>	<b>4,760</b>	<b>4,760</b>	<b>4,760</b>
Operational empty weight	608,600	628,630	623,690
Payload	350,000	350,000	350,000
Mission fuel	668,600	685,050	721,620
Reserves	43,300	42,880	44,020
<b>Takeoff gross weight</b>	<b>1,655,800</b>	<b>1,701,560</b>	<b>1,734,250</b>
<b>WEIGHTS COMPUTED BY STATISTICAL WEIGHT METHODS</b>			

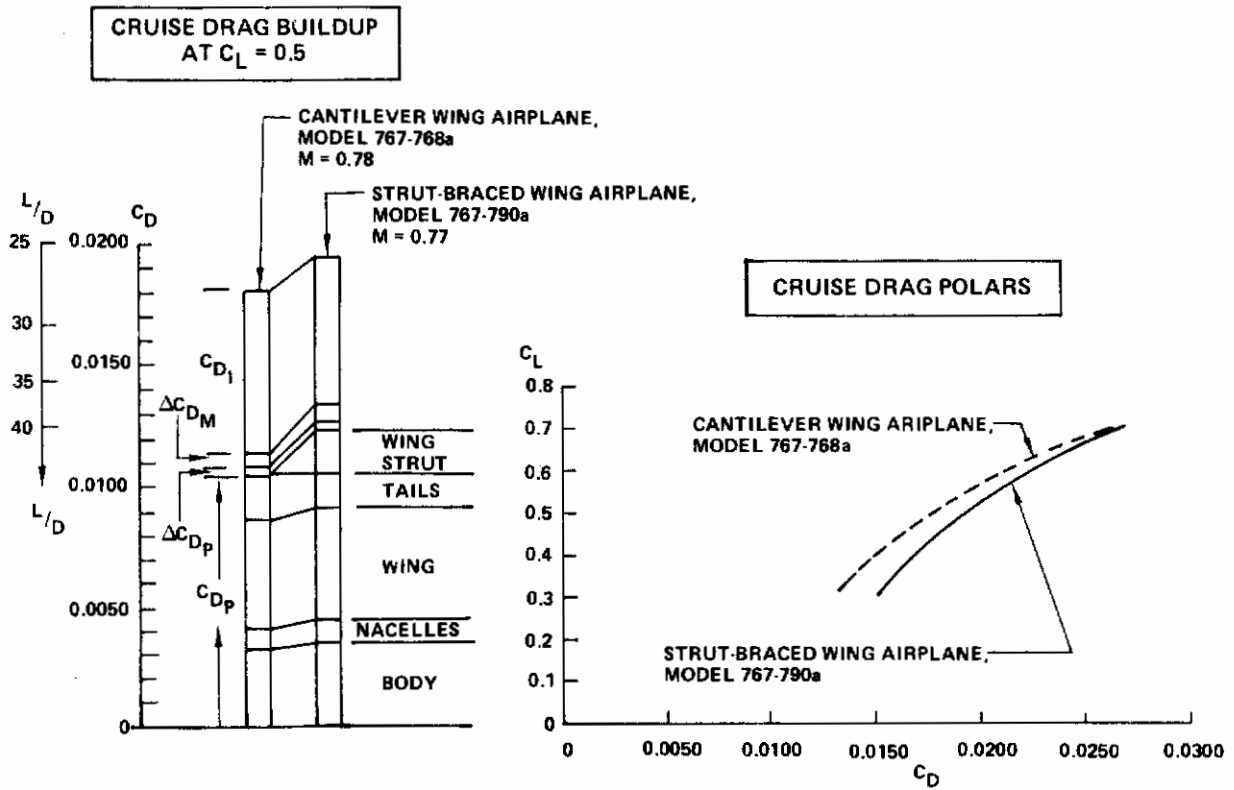


Figure 7 Cruise Drag Polar Comparison

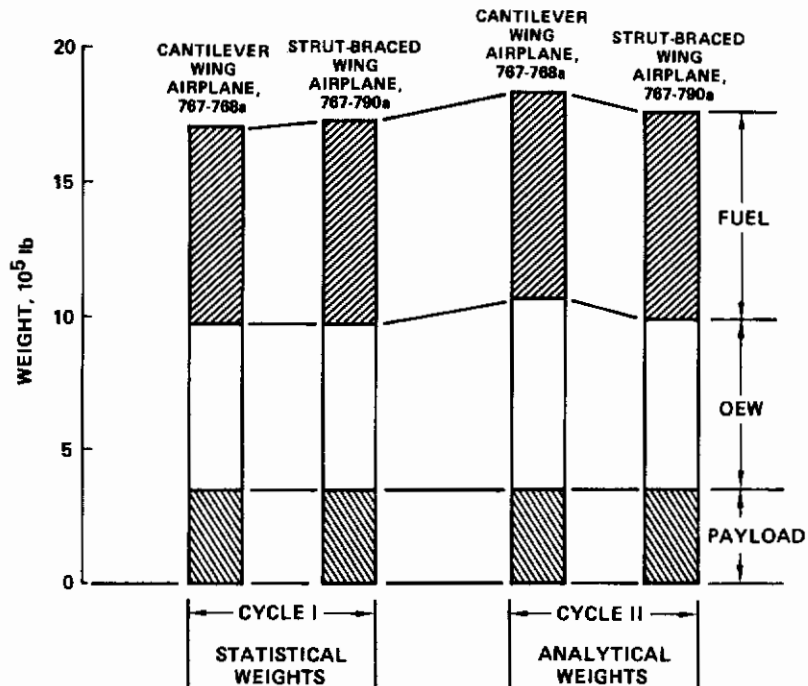


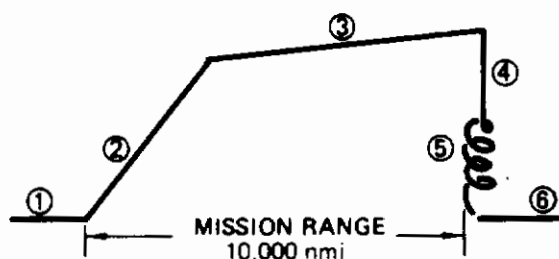
Figure 8 Gross Weight Comparison

## SECTION IV CONFIGURATION PERFORMANCE AND ECONOMICS

The cantilever wing and strut-braced wing configurations discussed in Section 3.0 were used to explore the potential impact of a braced wing on fuel, weight, life-cycle costs, and operating costs of a large military transport airplane.

### 1. MISSION RULES AND PERFORMANCE OBJECTIVES

Flight profiles and mission rules used in developing the study configurations are shown in Figure 9.



MISSION ELEMENT	ALLOWANCES
① START, TAXI, TAKEOFF	<ul style="list-style-type: none"> <li>● 5 min AT MAX CRUISE THRUST AT SEA LEVEL</li> <li>● 1 min AT MAX TAKEOFF THRUST AT SEA LEVEL</li> </ul>
② CLIMB	<ul style="list-style-type: none"> <li>● CLIMB FROM SEA LEVEL TO BEST CRUISE ALTITUDE AT MAX CLIMB POWER</li> </ul>
③ CRUISE-CLIMB	<ul style="list-style-type: none"> <li>● CRUISE-CLIMB AT BEST CRUISE ALTITUDE</li> </ul>
④ DESCENT	<ul style="list-style-type: none"> <li>● NO ALLOWANCE FOR FUEL, TIME, OR DISTANCE</li> </ul>
<b>RESERVES</b>	
⑤ LOITER	<ul style="list-style-type: none"> <li>● 30 min LOITER AT MAX ENDURANCE SPEED AT SEA LEVEL</li> </ul>
⑥ LANDING	<ul style="list-style-type: none"> <li>● LAND WITH 5% OF INITIAL MISSION FUEL</li> </ul>
<b>NOTES:</b>	
①	SFC IS INCREASED BY 5% THROUGHOUT THE MISSION
②	TAKEOFF DISTANCE IS BASED ON ALL ENGINES OPERATING <ul style="list-style-type: none"> <li>● TAKEOFF SPEED <math>\geq 1.2 V_s</math></li> <li>● DISTANCE TO 50-ft OBSTACLE <math>\leq 9,000</math> ft, SEA LEVEL <math>90^\circ F</math></li> <li>● ONE-ENGINE-OUT CLIMB REQUIREMENT <math>\geq 100</math> ft/min</li> </ul>
③	INITIAL CRUISE ALTITUDE $\geq 30,000$ ft
④	ENROUTE CRUISE SPEED $\geq 300$ kts

Figure 9 Flight Profile and Mission Rules

The following performance objectives and constraints have been used to size airplane configurations:

- Objectives:
  - Payload = 350,000 lb
  - Range = 10,000 nmi
  - Cruise Mach: determined by tradeoff studies
- Constraints:
  - Field length: 9,000 ft maximum

Range and payload objectives were the defined goals of the study to meet the long-range military airlift requirements. The 9,000 ft military critical field length requirements will allow operation from existing runways.

## 2. ENGINE/AIRFRAME MATCHING

The procedure used to size the airplane configurations includes the following steps. First, the detailed layouts of the cantilever wing configuration, Figure 3, and the braced-wing configuration, Figure 6, were evaluated to provide base point thrust, weight, aerodynamic, and flight control data. In addition, scaling relations were derived by further analyses to account for changes in wing size, engine size, and gross weight variations in the resizing cycle. A parametric engine/airframe matching method described in Reference 3 was used to determine the best combination of engine size, wing size, fuel requirements, and gross weight necessary to achieve the design mission objectives.

The design selection chart for the reference cantilever wing airplane is shown in Figure 10. This type of design chart parametrically shows the effect of thrust/weight ratio (T/W) and wing loading (W/S) on the airplane gross weight and block fuel requirements. Performance factors, such as takeoff field length (TOFL), initial cruise altitude capability (ICAC), and the ratio of the initial cruise lift coefficient capability to the lift coefficient for maximum lift/drag ratio ( $CL_R$ ) also are identified.

The minimum gross weight for the cantilever wing airplane requires a high wing loading of approximately 140 lb/ft<sup>2</sup>. With the high wing loading, the configuration could not meet the TOFL requirements. The minimum fuel burned arrangement, which requires a lower wing loading (110 lb/ft<sup>2</sup>), also does not meet the takeoff field requirements of 9,000 ft. The final design for the turbulent airplane was selected by considering the trade between fuel burned and gross weight along the TOFL = 9,000-ft constraint line (Figure 11). The

3. Wallace, R. E.: "Parametric and Optimization Techniques for Airplane Design Synthesis," Paper No. 7 in AGARD-LS-56, April 1972.

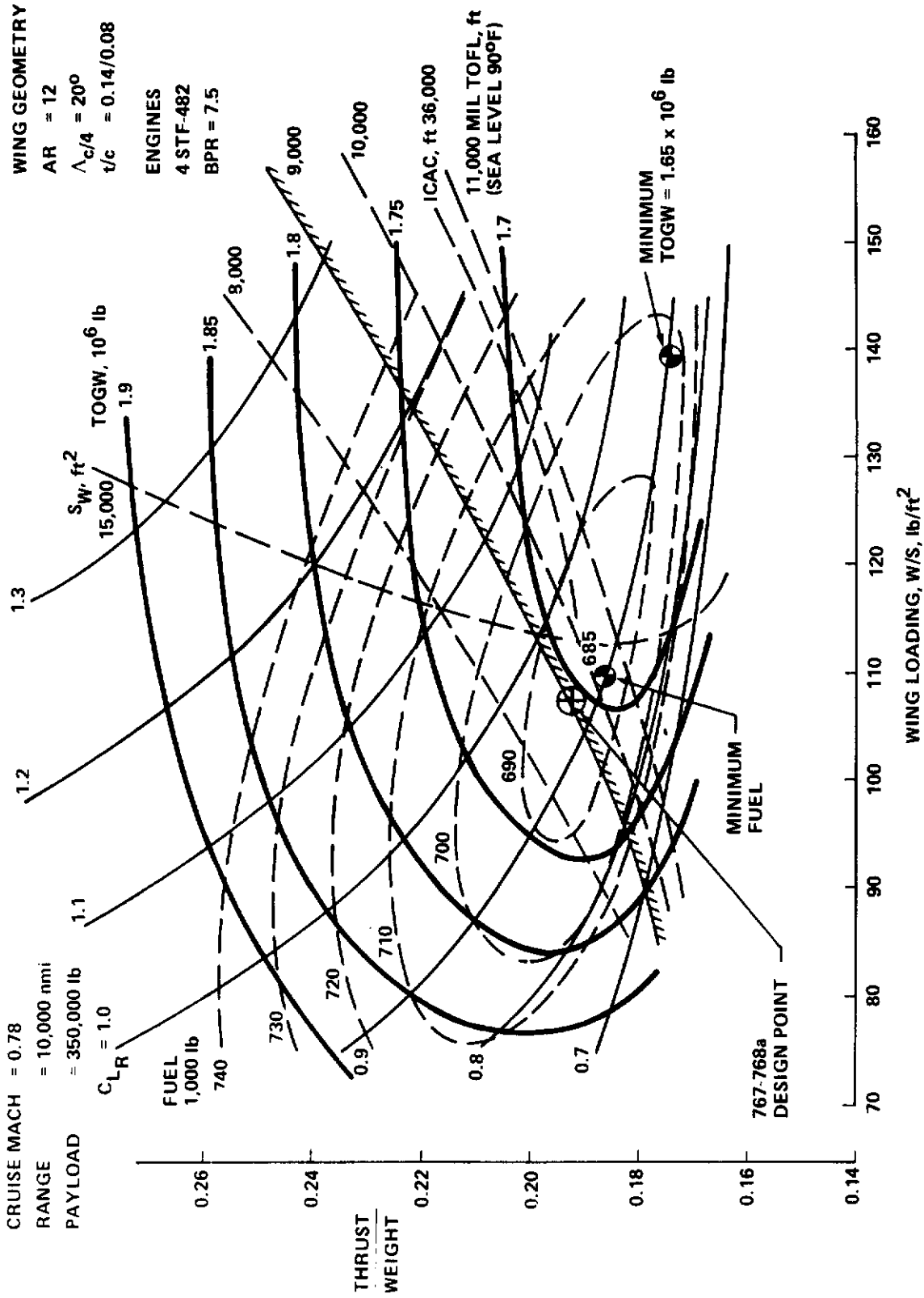


Figure 10 Cantilever Wing Airplane Engine/Airframe Matching



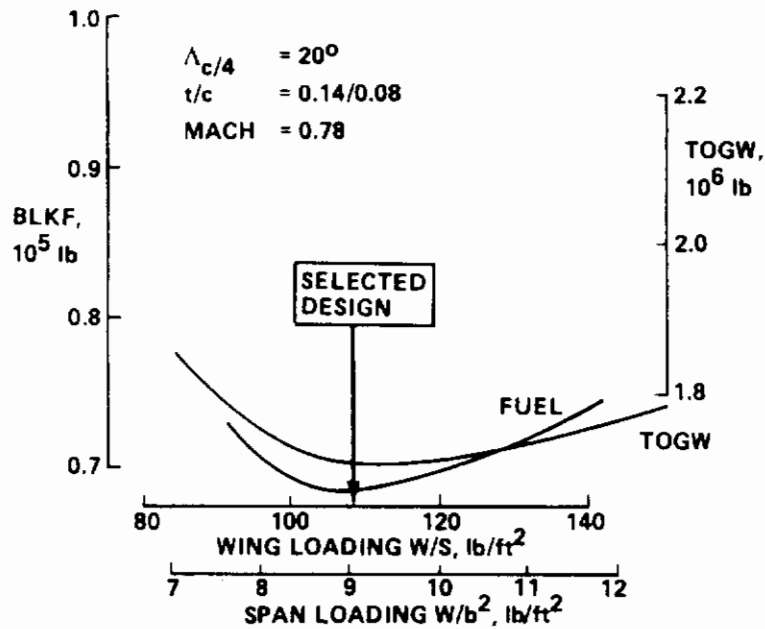


Figure 11 Cantilever Wing Airplane Design Selection

selected design, which has a wing loading of  $108 \text{ lb/ft}^2$ , has almost the minimum fuel and gross weight possible for this configuration.

The corresponding design selection chart for the strut-braced wing configuration is shown in Figure 12. The minimum gross weight configuration would require a wing loading in excess of  $140 \text{ lb/ft}^2$ . The design wing loading for minimum fuel is less than  $110 \text{ lb/ft}^2$ . Neither configuration meets the TOFL requirement. The final design selection for the strut-braced wing configuration, as shown in Figure 13, has a wing loading of  $120 \text{ lb/ft}^2$ .

### 3. PERFORMANCE COMPARISONS

Weight and performance characteristics of the cantilever wing and strut-braced wing configurations are summarized in Table 4. These results, which were derived using parametric statistical weights, indicate that the gross weight and fuel consumption of the strut-braced wing airplane are 2% and 5% greater, respectively, than the cantilever wing airplane.

The weight of the large-span wings of the study configurations is a major area of uncertainty. Consequently, sensitivity studies were made to determine the effects of variations of wing weight on the gross weight, fuel consumption, and size characteristics of the cantilever wing and strut-braced wing configurations. Results are shown in Table 5 as sensitivities expressed as percentage change in fuel, gross weight, etc. for a 10% change in base wing weight. A 10% variation in base wing weight changes fuel consumption and gross weight of the study configurations by approximately 4%.



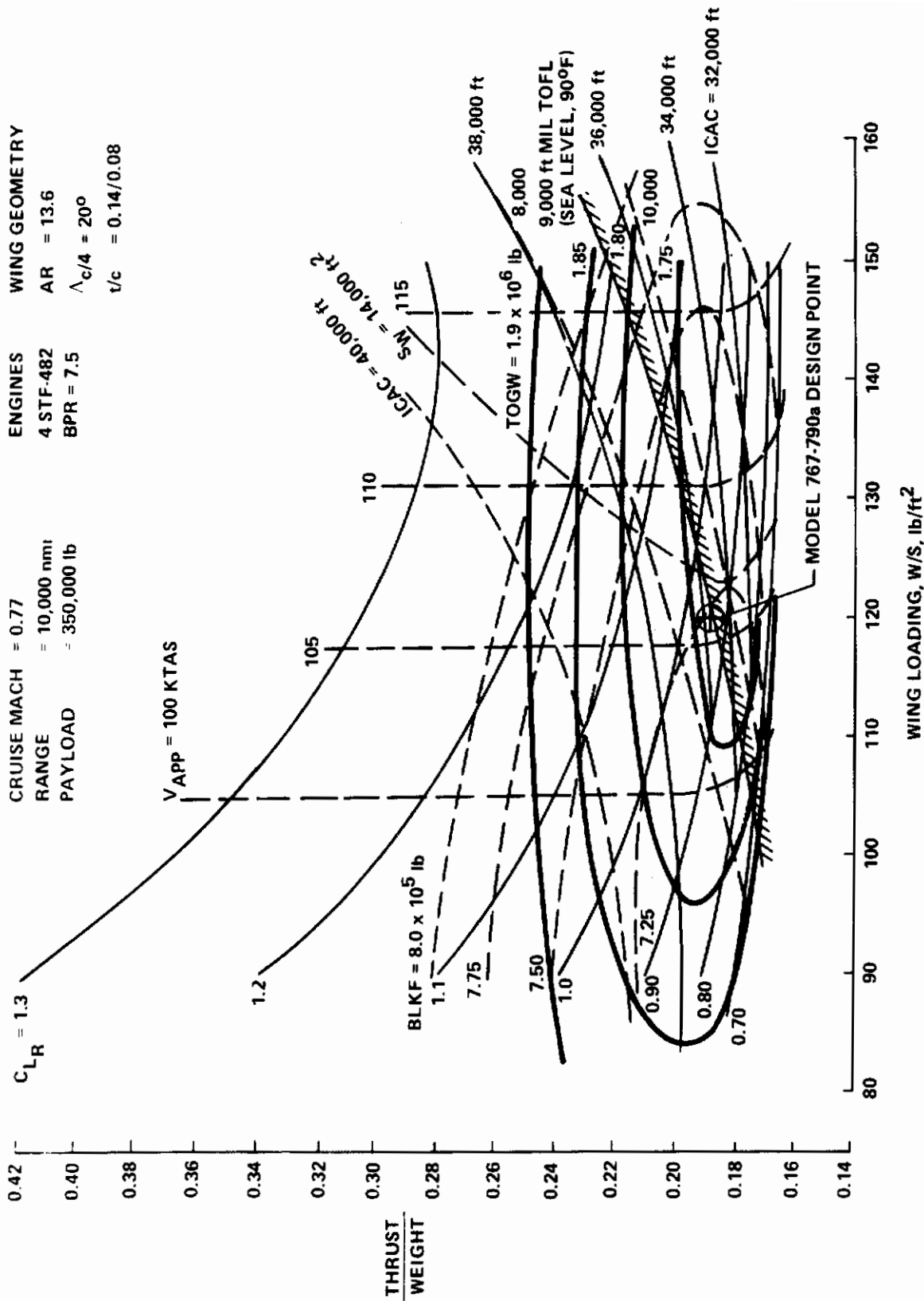


Figure 12 Strut-Braced Wing Airplane Engine/Airframe Matching

# Contrails

RANGE = 10,000 nmi      WING GEOMETRY  
PAYLOAD = 350,000 lb      AR = 13.4  
MACH = 0.77      t/c = 0.14/0.08  
MIL TOFL = 9,000 ft       $\Lambda_{c/4} = 25^\circ$

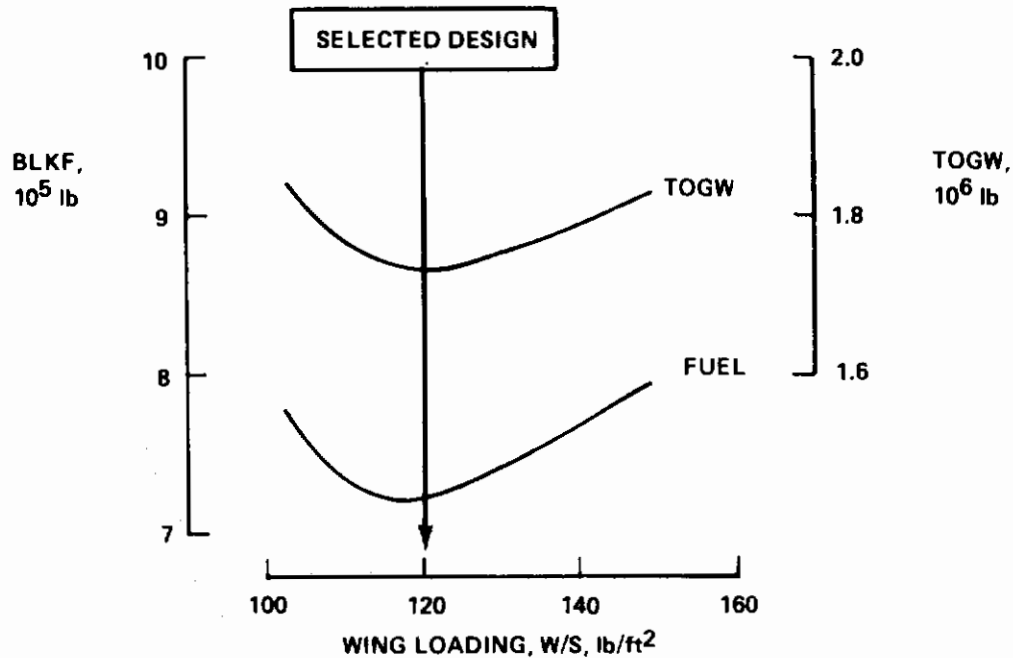


Figure 13 Strut-Braced Wing Design Selection

Detailed structural analyses described in Section VI were used to develop more accurate analytical weight estimates of the base cantilever wing and strut-braced wing. Additional evaluations were made to determine the effect of wing thickness distribution on wing weight. The cantilever wing configuration and the strut-braced wing configuration were resized with the base wing weights determined by the structural analyses.

Effects of wing thickness on the gross weight, fuel consumption, and OEW of the cantilever wing configuration are shown in Figure 14. Results obtained with the statistical weights indicate that the 0.14/0.08 thickness distribution minimizes fuel burned, gross weight, and OEW. Results of the analytical weight evaluation indicate that the weight of the thinnest wing is significantly heavier than indicated by the statistical weights. The statistical weight and analytical weight evaluations of the thickest wings were nearly equal. Consequently, results obtained with the analytical weights indicate that minimum fuel consumption is obtained with the thin wing (0.14/0.08). Thicker wings, however, will reduce gross weight and empty weight.

The analytical weight evaluations of the strut-braced wing indicate that the wing weight is higher than had been predicted by the statistical weights. The relative weight increase was not as great as for the comparable thickness (0.14/0.08) cantilever wing. Hence, using the

Table 4 Final Sized Airplane Characteristics, Models 767-768a and 767-790a

ITEM	UPDATED CANTILEVER WING AIRPLANE, MODEL 767-768a		STRUT-BRACED WING AIRPLANE, MODEL 767-790a	
	Design mission	Payload, lb	350,000	
	Range, nmi	10,000		
Weights, lb	TOGW	1,701,560	1,734,250	
	OEW	628,230	623,680	
	Block fuel	685,050	721,620	
	Reserves	42,880	44,040	
Wing	Area, ft <sup>2</sup>	15,755	14,450	
	AR	12	13.4	
	t/c Inboard/outboard	0.14/0.08	0.14/0.08	
	$\Lambda_c/4$ , deg	20	20	
	W/S, lb/ft <sup>2</sup>	108.0	120.0	
Engine	Engine type/no./BPR	STF 482/4/7.5		
	SLST, lb	80,720	81,770	
	T/W, lb/lb	0.190	0.189	
Performance	Mach	0.78	0.77	
	ICAC, ft	36,400	35,300	
	h <sub>AVE</sub> , CRU, ft	41,000	39,900	
	L/D <sub>CRU</sub>	27.8	26.7	
	SFC <sub>CRU</sub> , lb/hr/lb (a)	0.603	0.603	
	V <sub>APP</sub> , keas	102.6	105.8	
TOFL (Mil), ft	9,000	9,000		

(a) Includes 5% military mission fuel allowance

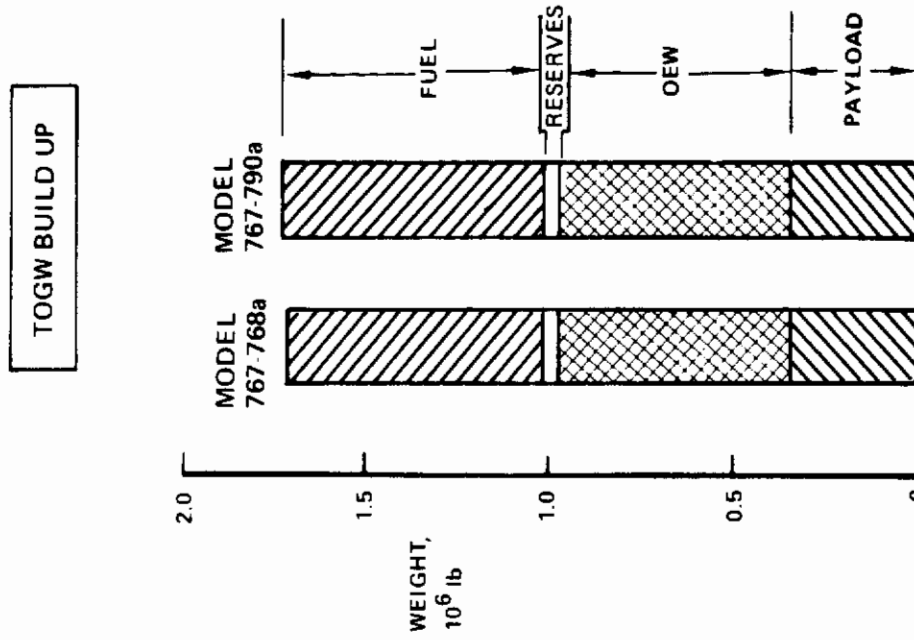


Table 5 Airplane Sensitivities to Wing Weight Variations

QUANTITY	PERCENT CHANGE FOR A 10 PERCENT INCREASE IN WING WEIGHT	
	CANTILEVER WING AIRPLANE AR = 12 t/c = 0.14/0.08	STRUT-BRACED WING AIRPLANE AR = 13.4 t/c = 0.14/0.08
Empty weight:		
–Uncycled	3.3	3.2
–Cycled	7.3	6.3
Gross weight	4.2	3.4
Fuel burned	3.4	2.6
Thrust required	4.1	3.4
Wing area	4.2	3.5

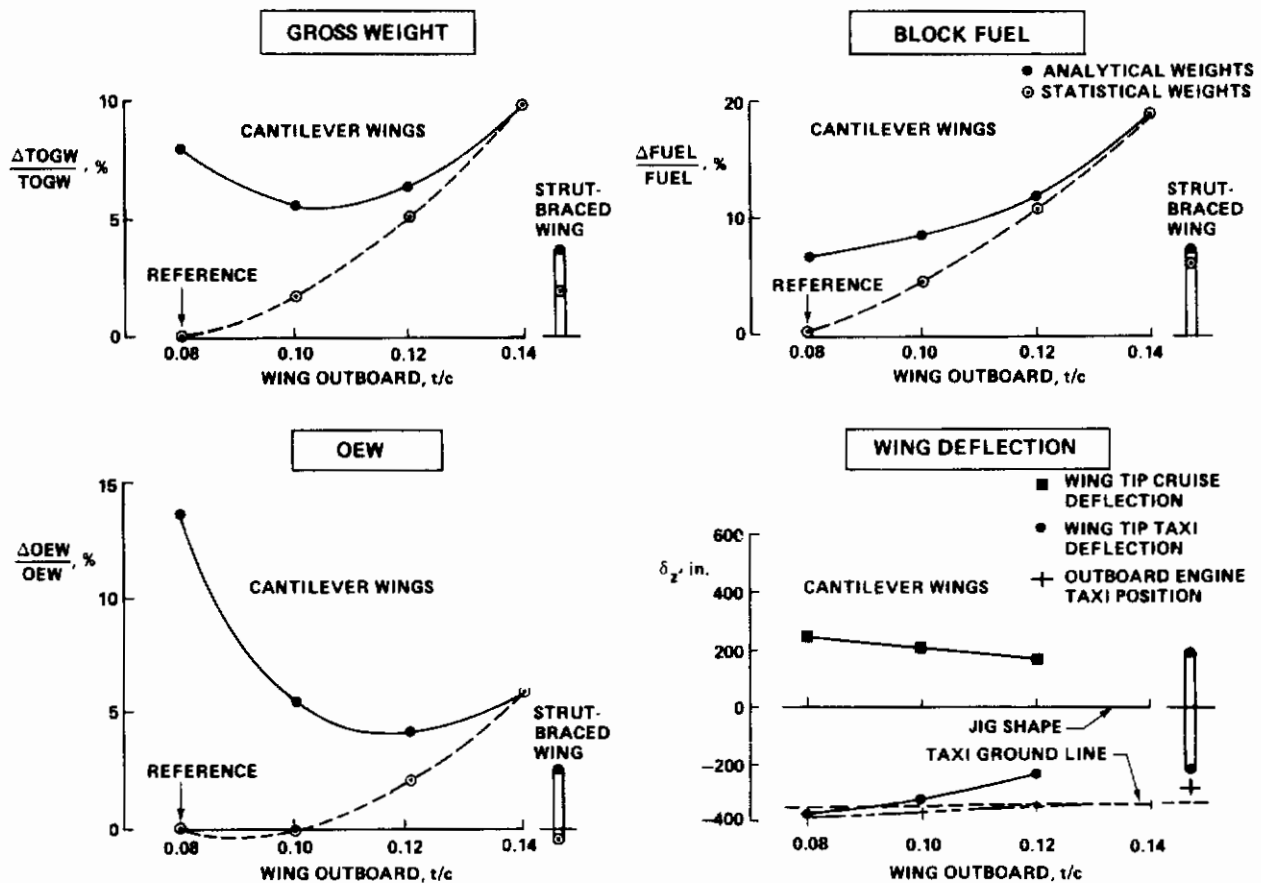


Figure 14 Large-Span Wing Comparisons

results of the more accurate analytical weights, the strut-braced wing requires less fuel (-1.6%), lower gross weight (-1.8%), and lower empty weight (-3%), than the cantilever wing with the "best" thickness distribution (0.15/0.10). In addition, the cruise Mach number of the strut-braced wing would be slightly faster than the thicker (0.15/0.10) cantilever wing.

The results in Figure 14 also indicate that the strut-braced wing is effective in reducing wing taxi deflections.

#### 4. LIFE-CYCLE COSTS AND OPERATING COSTS COMPARISONS

Economic analyses were made to determine the 20-year life-cycle costs and surge condition operating costs of the cantilever wing and the strut-braced wing configuration. Ground rules for the life-cycle cost calculations are summarized in Figure 15. The low utilization rate of 1,080 flying hours per airplane used for the life-cycle cost calculations is about one-third to one-quarter that of the annual usage of commercial transports.

Relative life-cycle costs are shown in Figure 15. Table 6 contains the life-cycle cost elements. Production costs are the major cost items. Fuel costs make up a relatively small portion of the total life-cycle costs, because of the airplane low-utilization rate.

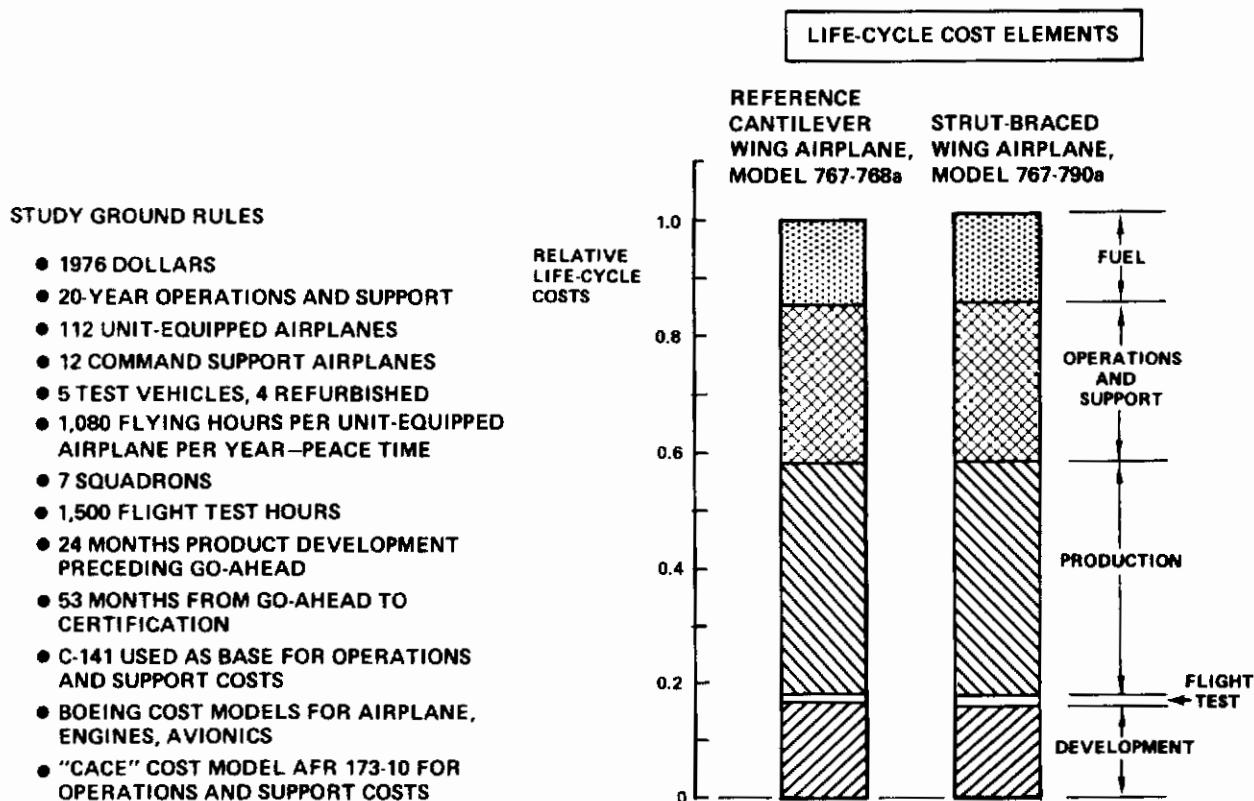


Figure 15 Twenty-Year Life-Cycle Cost Comparisons

**Table 6 Twenty-Year Life-Cycle Cost Elements, Based on Statistical Weights**

COST ELEMENT	CANTILEVER WING AIRPLANE, 767-768a	STRUT-BRACED WING AIRPLANE, 767-790a
Development	\$ 4,391.843	\$ 4,170.731
Airframe	1,105.061	1,115.144
Engines	55.000	55.000
Avionics		
Flight test airplane		
Airframe	290.239	289.734
Engines	5.894	5.947
Avionics	2.200	2.200
Flight test operations	221.054	218.506
<b>Total</b>	<b>\$ 6,071.291</b>	<b>\$ 5,857.262</b>
Production		
Airframe	\$12,228.037	\$12,520.274
Engines	730.814	737.482
Avionics	272.800	272.800
<b>Total</b>	<b>\$13,231.651</b>	<b>\$13,530.556</b>
Support investment	\$ 1,984.748	\$ 2,029.583
Operations and support		
AGE, spares, mods	\$ 1,623.160	\$ 1,647.380
Military pay and allowances	2,012.080	2,012.080
Depot maintenance	1,974.980	1,982.680
Fuel	4,910.920	5,138.420
Pipeline support	307.300	307.300
Other	1,039.360	1,039.360
<b>Total</b>	<b>\$11,867.800</b>	<b>\$12,127.220</b>
<b>Total life-cycle cost</b>	<b>\$33,155.490</b>	<b>\$33,544.621</b>

NOTE: COSTS IN 1977 \$, \$ MILLIONS

Operating costs were determined for a surge condition with a higher utilization rate of 10 flying hours per day per airplane for a 60-day period. Ground rules and results are shown in Figure 16 and Table 7. Fuel costs comprise a major portion of the operating costs.

The cost comparisons in Figures 15 and 16, and in Tables 6 and 7, indicate that operating costs and life-cycle costs of the cantilever wing configuration are very slightly less than for the strut-braced wing configuration. These results were obtained using the statistical weight evaluations. The analytical weight evaluations described in Section VI indicate that the gross weights of the strut-braced wing configuration are less than those of the cantilever wing configuration. Consequently, the operating and life-cycle costs of the strut-braced wing configuration would be slightly less than those of the cantilever wing airplane.

However, to fully determine the performance and economic potential of the strut-braced wing configuration, coordinated detailed structural and aerodynamic studies are necessary.



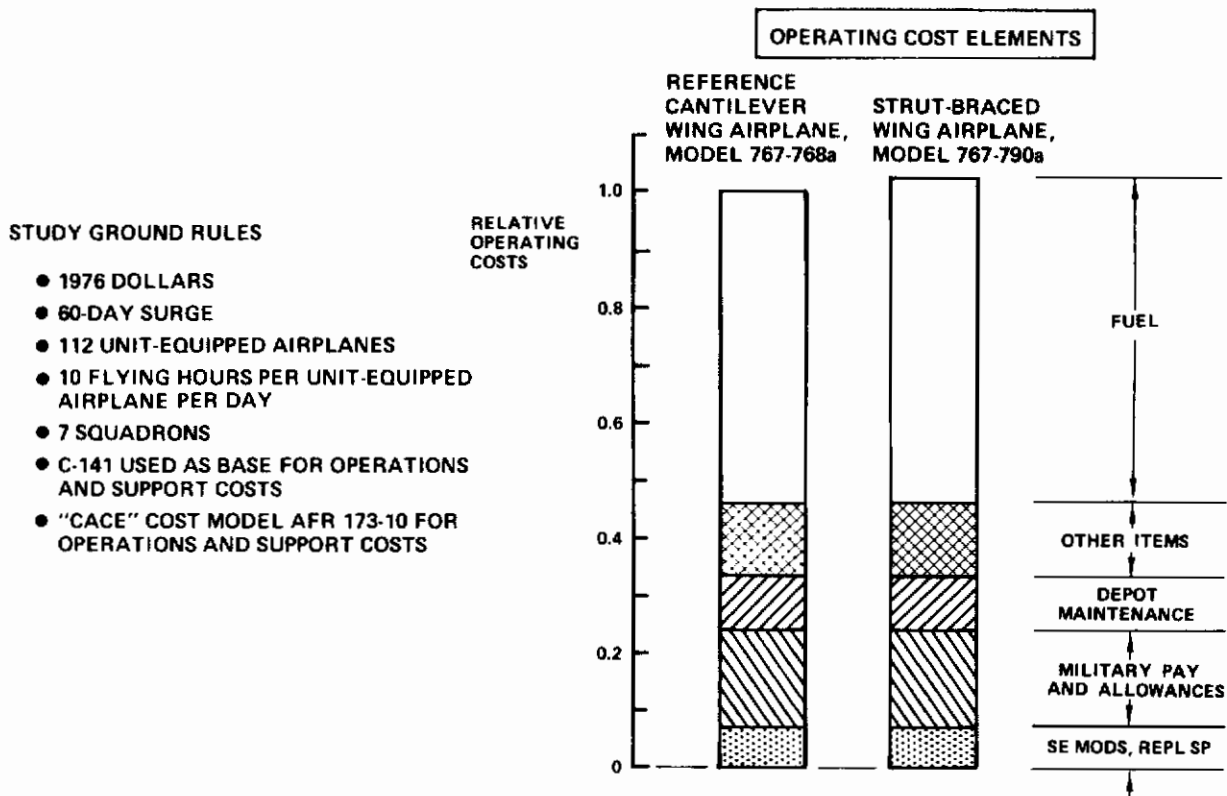


*Figure 16 Surge Condition Operating Cost Comparisons*

*Table 7 Surge Condition Cost Elements, Based on Statistical Weights*

COST ELEMENT	CANTILEVER WING AIRPLANE, 767-768a	STRUT-BRACED WING AIRPLANE, 767-790a
Operations and support		
SE, mods, repl spares	\$ 17.504	\$ 17.703
Military pay and allowances	42.992	42.992
Depot maintenance	24.229	24.292
Aviation fuel	136.416	142.734
Pipeline support	5.411	5.411
Other	<u>27.114</u>	<u>27.114</u>
<b>TOTAL</b>	<b>\$253.666</b>	<b>\$260.246</b>

NOTE: COST IN 1977 \$, \$ MILLIONS

# *Contrails*



## SECTION V

### CANTILEVER WING GEOMETRY/CRUISE SPEED OPTIMIZATION STUDY

A wing geometry/cruise speed parametric study was conducted to optimize the cantilever wing configuration. The technique used consists of the five sequential steps shown in Figure 17. The first step involves the definition of the study variables. Primary variables included:

- Wing inboard/outboard thickness/chord ratios: 0.14/0.08; 0.15/0.10;  
0.16/0.12; 0.17/0.14
- Wing aspect ratio: 8, 10, 12, 14
- Sweep  $\Lambda_{c/4}$ :  $10^{\circ}$ ,  $20^{\circ}$ ,  $25^{\circ}$ ,  $30^{\circ}$

Secondary variables included:

- Wing loading:  $W/S = 60-120 \text{ lb/ft}^2$
- Thrust/weight ratio:  $T/W = 0.10-0.30$
- Mach number:  $M = 0.70-0.85$
- Optimum cruise altitude

Design constraints included:

- Range = 10,000 nmi
- Payload = 350,000 lb
- Takeoff field length  $\leq 9,000 \text{ ft}$

Principal design figures of merit include:

- Fuel burned
- Takeoff gross weight
- Productivity

In the second step, the method of orthogonal Latin squares was used to select 16 wing designs out of the possible 64 combinations of primary design variables. This design selection procedure provides an unbiased choice of the primary variables, and is a uniform representation of the design space.

Each of the 16 selected designs was evaluated and sized by the engine/airframe matching technique described in Paragraph IV.2. This step provides specific values of the optimized secondary variables and figures of merit.

A forward step regression analysis method was then used to construct approximating functions to represent the relationship between the primary independent variables and each

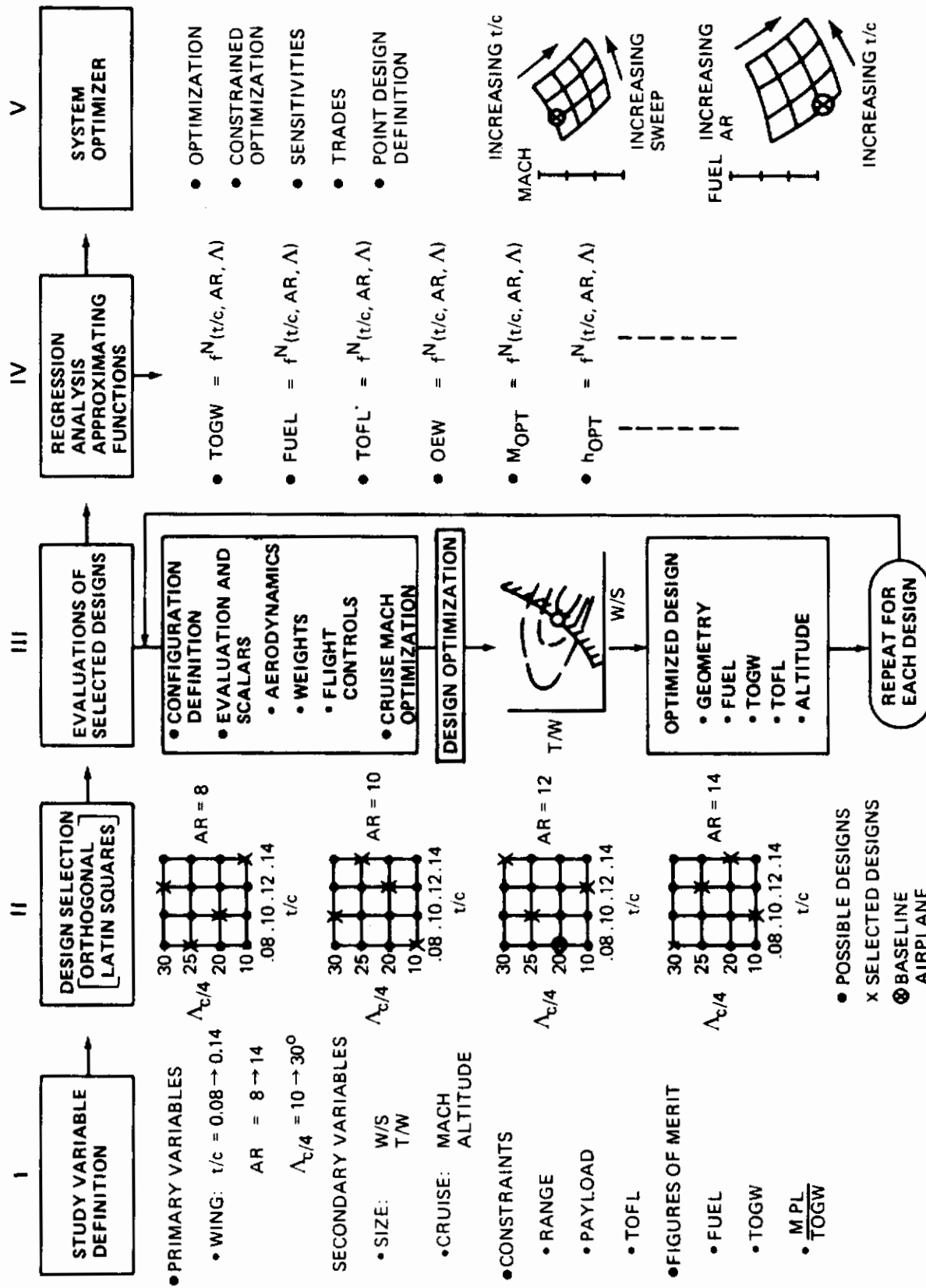


Figure 17 Wing Parametric Optimization Study

dependent variable, including the constraints and the figures of merit. The generalized form of the regression equation is:

$$\begin{aligned} \text{Dependent variable} &= C_1 + C_2(\text{AR}) + C_3(t/c) + C_4(\Lambda_{c/4}) && \text{(Linear)} \\ &+ C_5(\text{AR} \times t/c) + C_6(\text{AR} \times \Lambda_{c/4}) + C_7(t/c \times \Lambda_{c/4}) && \text{(Cross products)} \\ &+ C_8(\text{AR})^2 + C_9(t/c)^2 + C_{10}(\Lambda_{c/4})^2 && \text{(Squares)} \end{aligned}$$

The stepwise regression analysis retains only the significant terms in the equation. The resulting equations are not laws of nature, but rather represent a statistically derived data enrichment procedure.

The approximating functions can then be used in a powerful nonlinear optimizer to conduct constrained or unconstrained optimization, sensitivity, and trade studies. This parametric optimization process is described in Reference 4.

## 1. OPTIMIZATION RESULTS

The design selections for each of the 16 configurations that were analyzed are shown in Figures 18 through 21. The selected designs all were close to the constrained minimum fuel configuration, and also to the constrained minimum gross weight configurations. The corresponding wing loadings vary from  $W/S = 85$  to  $110 \text{ lb/ft}^2$ .

Results of the wing planform/cruise speed optimization study are shown in Figures 22 through 30. These results illustrate the impact of the wing planform geometry on the cruise Mach number, lift/drag ratio, range factor, thrust/weight ratio, fuel requirements, TOGW, and productivity of the cantilever wing configurations. The surface fit equations are shown to be a good representation of the initial baseline configuration and the additional 15 study configurations.

The spanwise variation of thickness/chord ratio is shown in Figure 22. The thickness/chord ratio referred to in the subsequent figures corresponds to the thickness/chord ratio on the outboard portion of the wing. In all cases, the inboard thickness/chord is greater than that outboard on the wing.

The effects of planform geometry on lift/drag ratio and cruise range factor are shown in Figures 23 and 24 respectively. Aspect ratio and wing thickness have a powerful effect on the aerodynamic efficiency of the airplane. High aspect ratios, as shown in Figure 25, lower the required thrust/weight ratio significantly. Characteristics of the optimum wing planforms

4. Healy, M. J.; Kowalik, J. S.; and Ramsay, J. W.: "Airplane Engine Selection by Optimization on Surface Fit Approximations." Journal of Aircraft, Vol. 12, No. 7, July 1975.

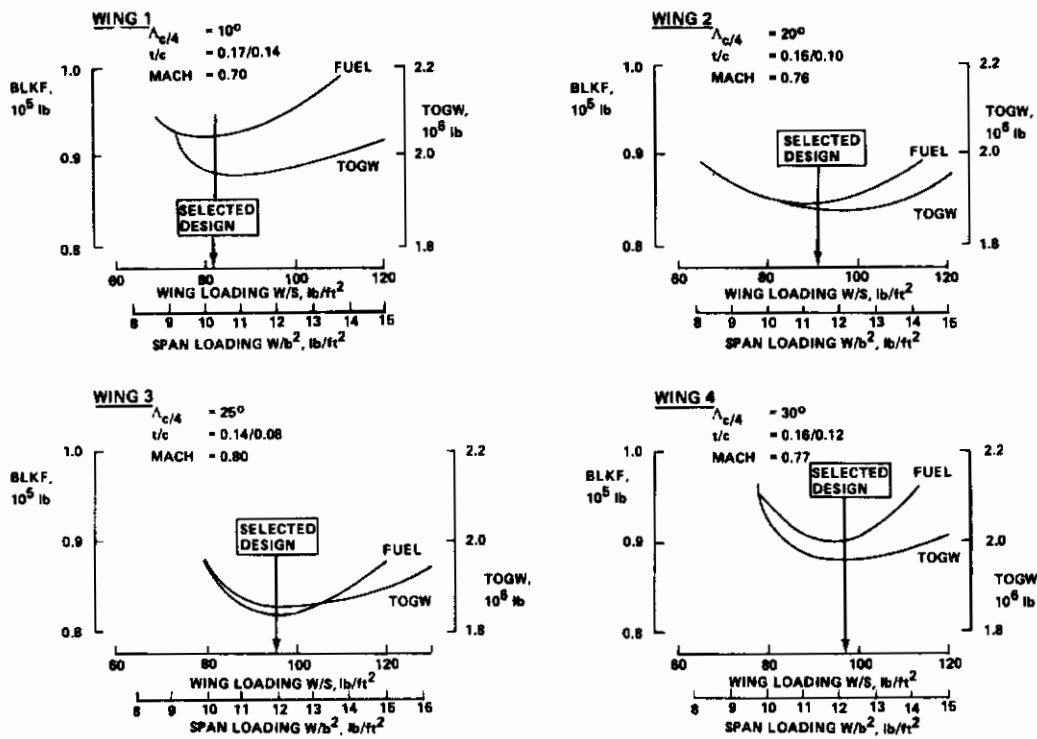


Figure 18 Configuration Selections for the Aspect Ratio 8 Wing Designs

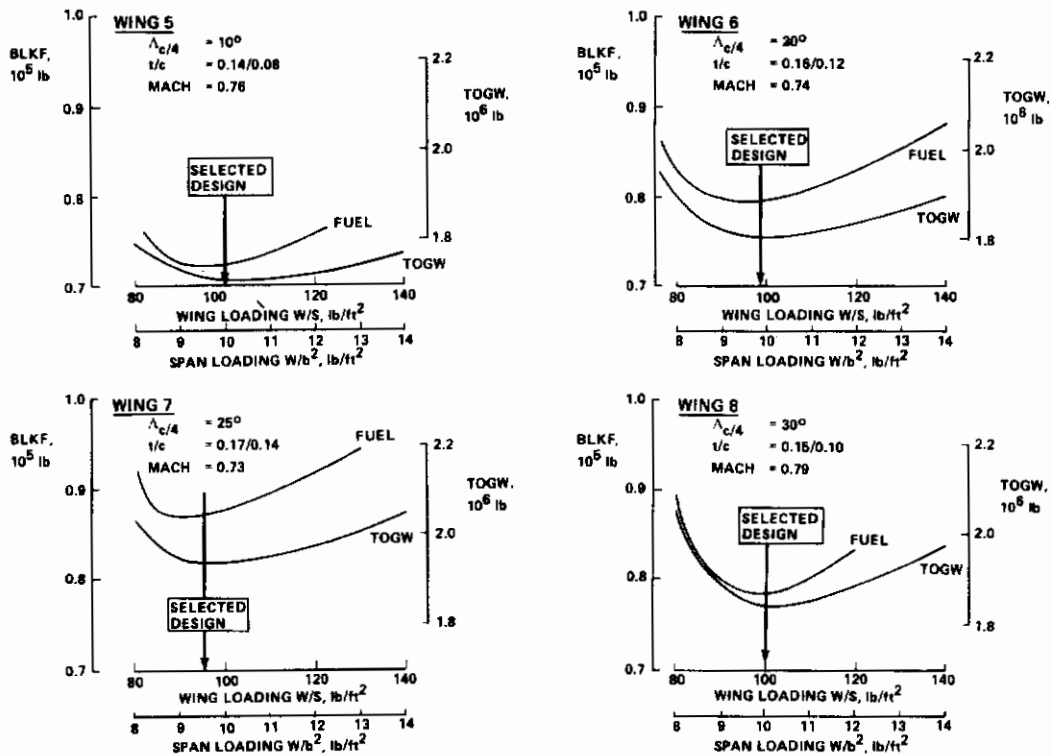


Figure 19 Configuration Selections for the Aspect Ratio 10 Wing Designs

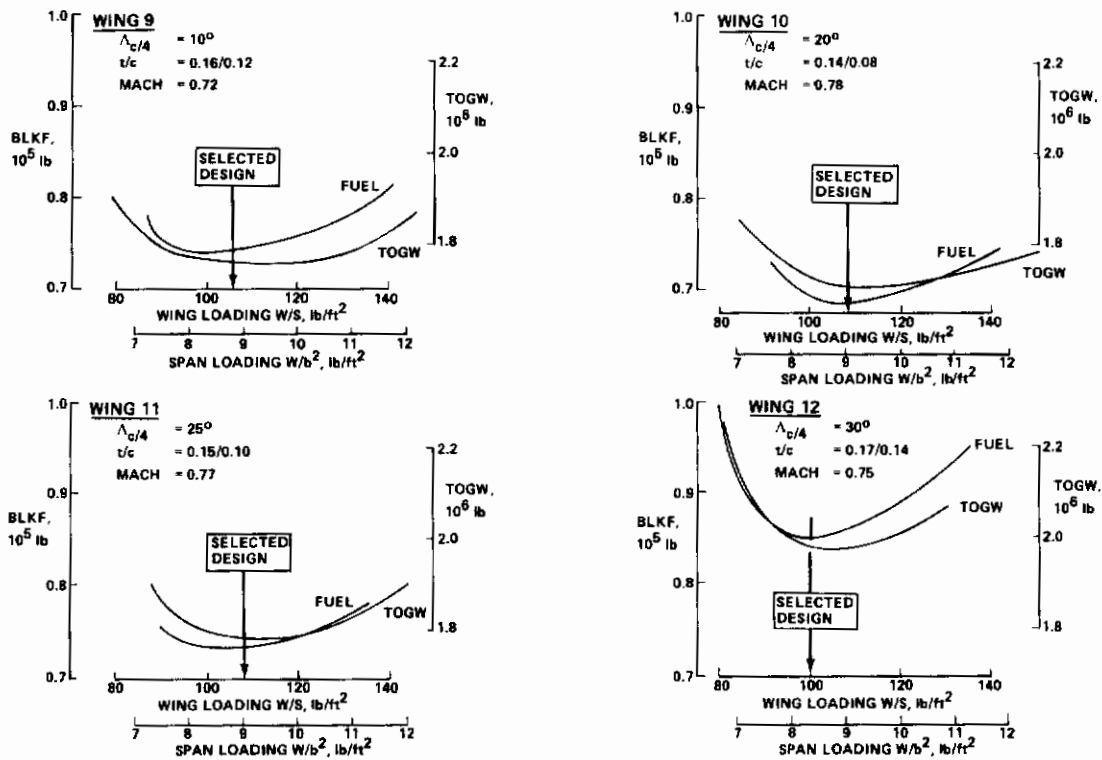


Figure 20 Configuration Selections for the Aspect Ratio 12 Wing Designs

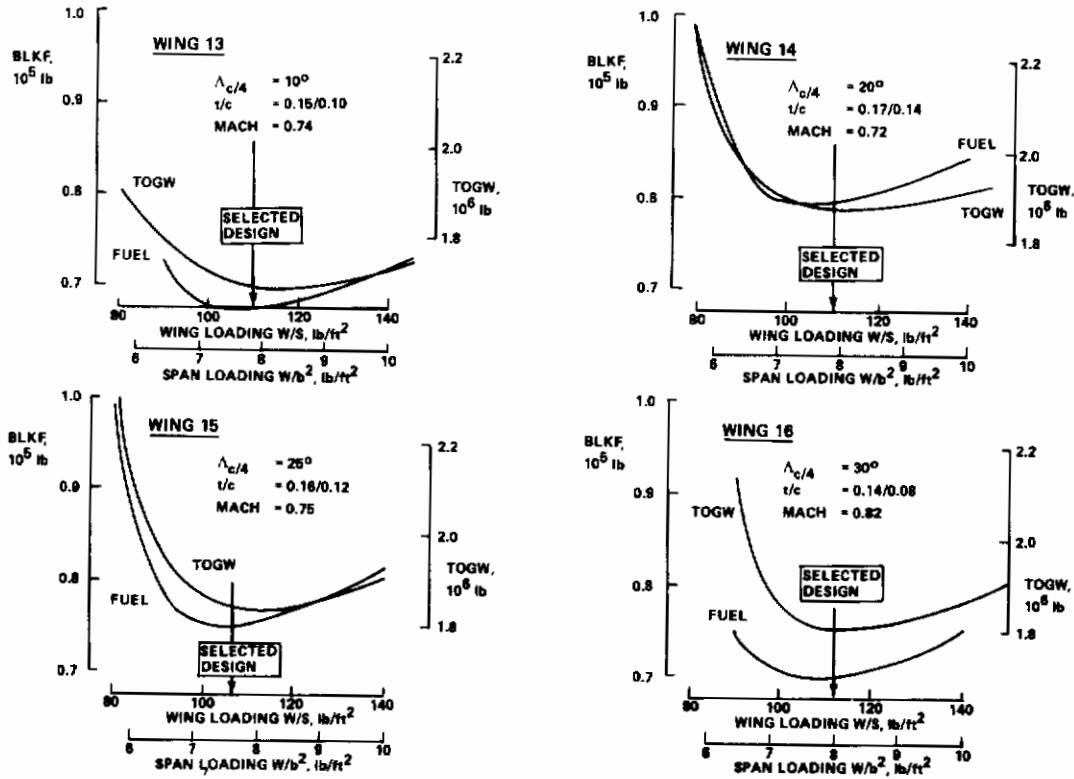


Figure 21 Configuration Selections for the Aspect Ratio 14 Wing Designs

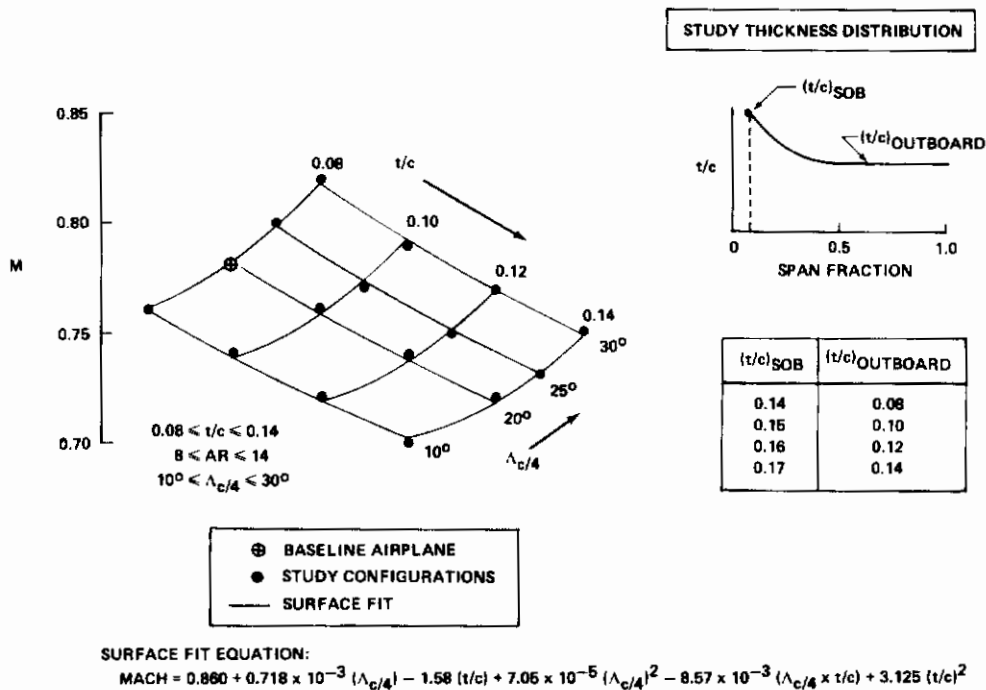


Figure 22 Cruise Mach Number

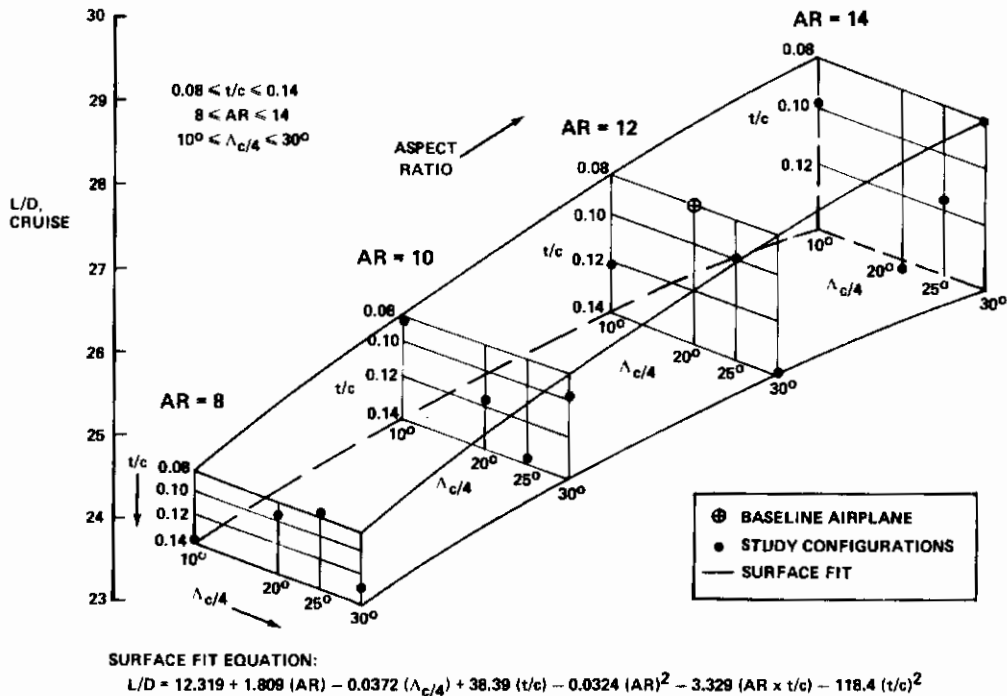


Figure 23 Cruise Lift/ Drag Ratio



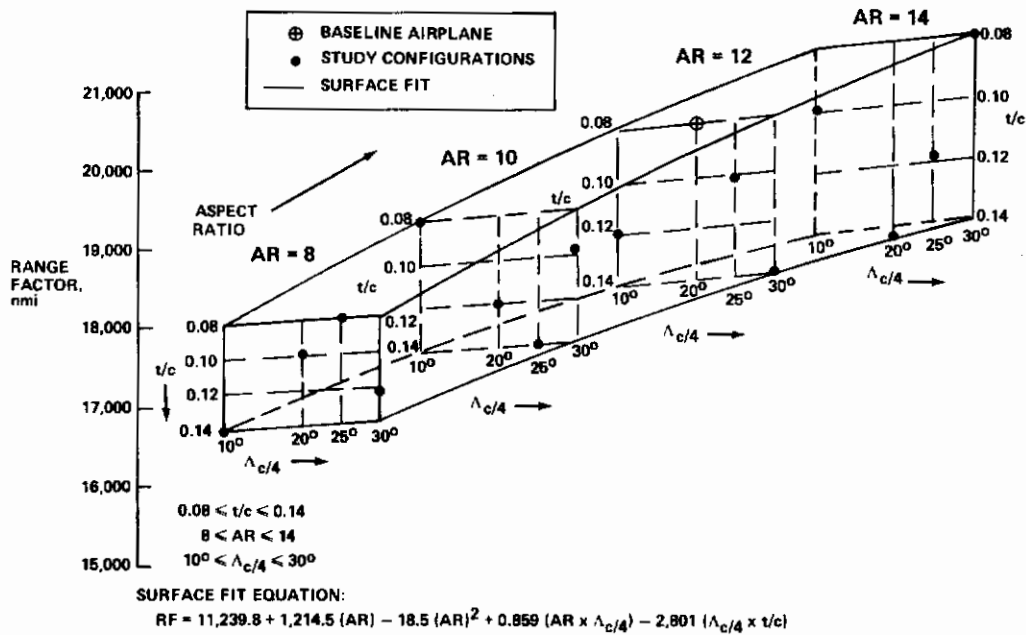


Figure 24 Cruise Range Factor

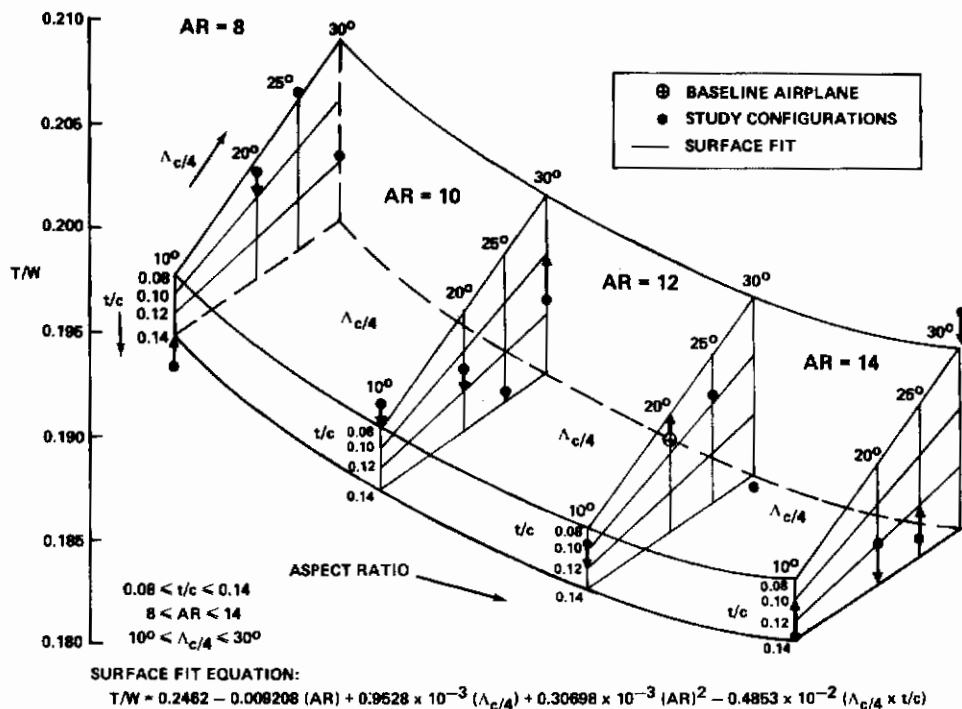


Figure 25 Thrust/Weight Ratio

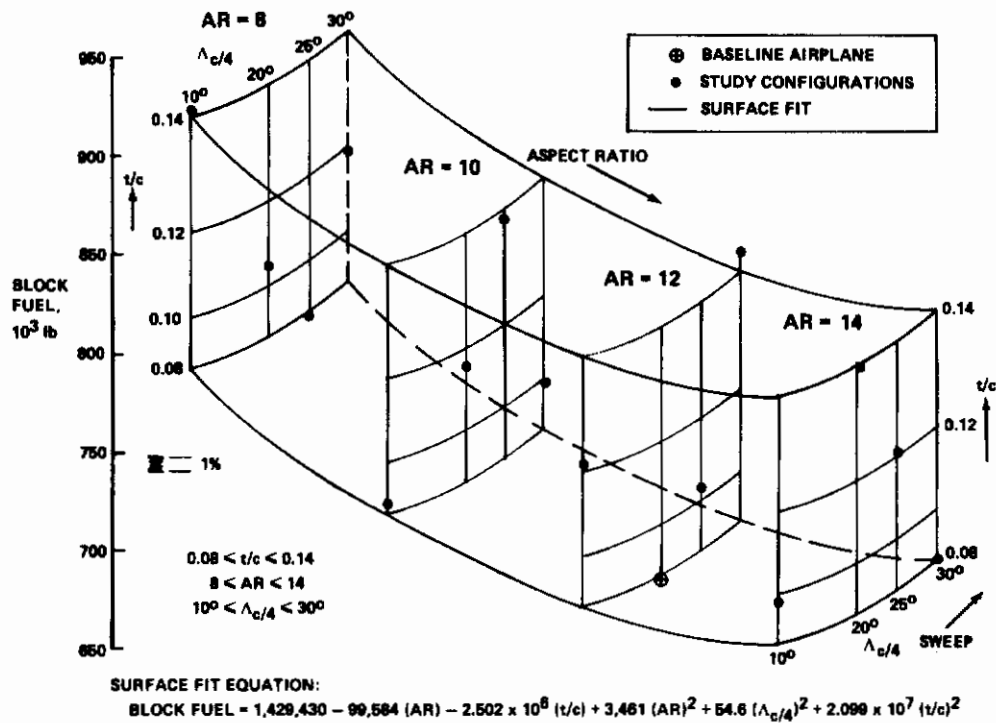


Figure 26 Block Fuel

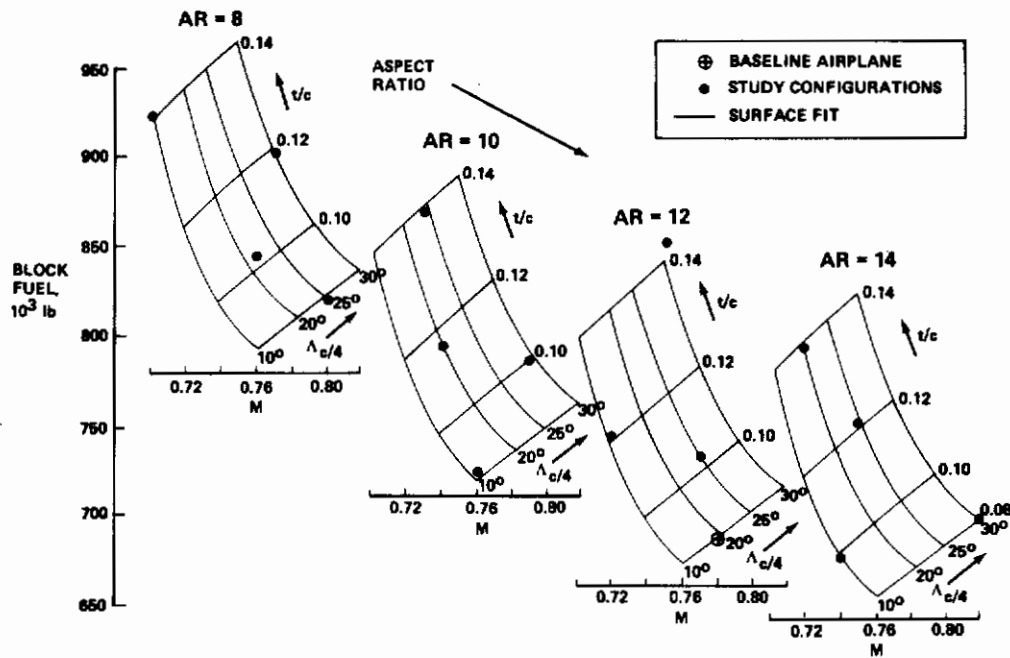


Figure 27 Effect of Cruise Mach on Block Fuel



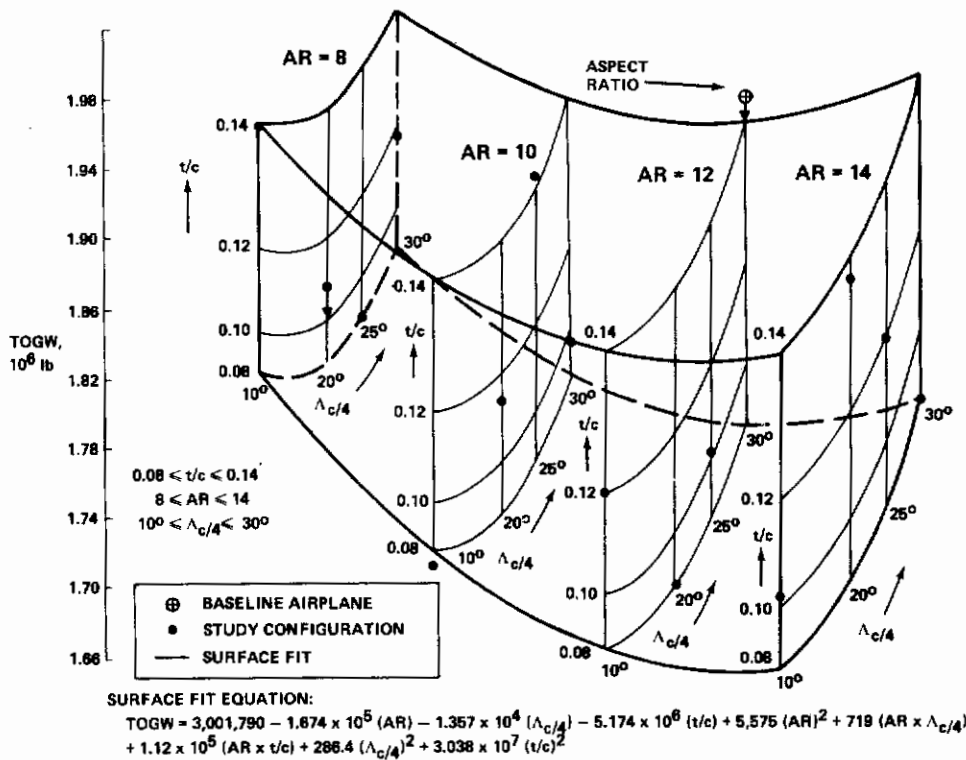


Figure 28 Takeoff Gross Weight

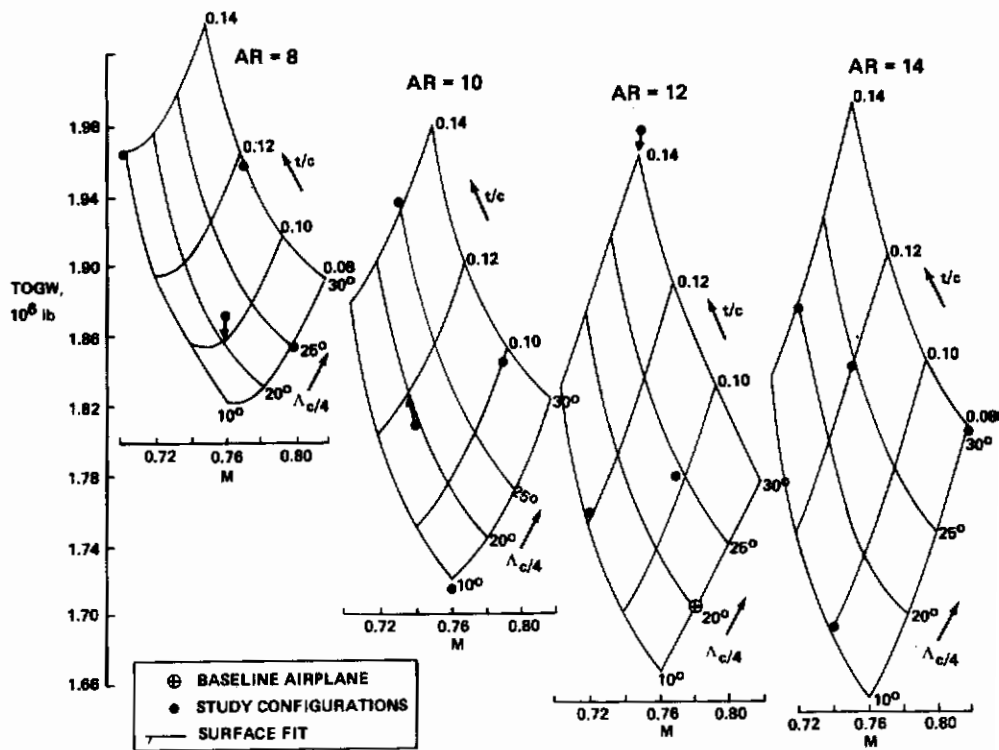
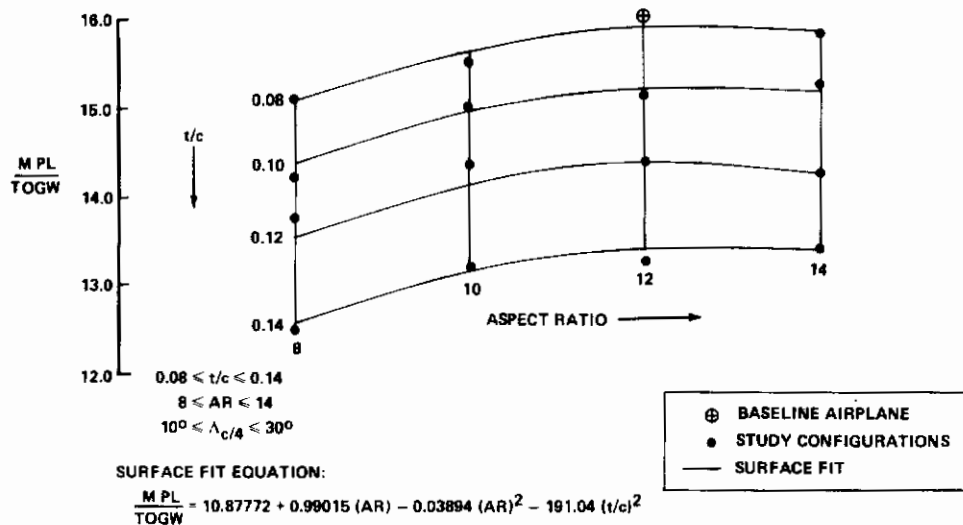


Figure 29 Cruise Mach Effect on TOGW



*Figure 30 Productivity (MPL/TOGW)*

with minimum fuel, minimum gross weight, or maximum productivity as figures of merit are summarized in Table 8. The sensitivities of the optimum configurations to variations in each of the primary design variables over the range of values studied are shown in Table 8.

The optimum planform with minimum fuel as the figure of merit has the highest aspect ratio, and the lowest sweep and thickness/chord ratio, (Figures 26 and 27). This results in a cruise Mach number of 0.76. The sensitivity data (Table 8) show that achieving a high aspect ratio and low thickness/chord ratios are most important. Reducing the aspect ratio from 14 to 8 would increase the fuel consumption by 21%. Increasing the wing thickness/chord ratio from 8% to 14% would increase fuel consumption by 20%. Wing sweep is seen to be a less important parameter.

The minimum fuel consumption configuration is also the minimum gross weight configuration (Figures 28 and 29). The optimum wing aspect ratio decreases as either wing thickness or wing sweep are increased. The sensitivity data show that gross weight varies by approximately 10% for changes in either aspect ratio, thickness/chord ratio, or wing sweep over the range of values of these variables that was considered. The wing aspect ratio could be reduced from 14 to 12, however, without significantly affecting the gross weight.

The maximum productivity configuration has a low thickness/chord ratio and an aspect ratio of 12.7 (Figure 30). Low thickness/chord ratio is most important in achieving high productivity. Wing sweep did not significantly affect productivity, since the gross weight variations with sweep were proportional to the Mach number changes.

## 2. CANTILEVER WING CONFIGURATION SELECTION

Results of the wing geometry/cruise speed optimization indicate that a wing planform having an aspect ratio of 14, thickness ratio variation of 0.14/0.08 (inboard/outboard), and sweep of

**Table 8 Optimum Configurations and Design Sensitivities**

**OPTIMUM CONFIGURATIONS**

FIGURE OF MERIT	AR	t/c	$\Lambda_{c/4}$	MACH
Minimum fuel	14 (MAX)	0.08 (MIN)	10° (MIN)	0.76
Minimum TOGW	14 (MAX)	0.08 (MIN)	10° (MIN)	0.76
Maximum $\frac{M PL}{TOGW}$	12.7	0.08 (MIN)	Not significant	

Design space:  $8 \leq AR \leq 14$   
 $0.08 \leq t/c \leq 0.14$   
 $10^\circ \leq \Lambda_{c/4} \leq 30^\circ$

**DESIGN SENSITIVITIES**

CONFIGURATION	PRIMARY FIGURE OF MERIT:	CHANGE (%)	DESIGN VARIABLE RANGE
Minimum fuel A/P	Fuel:	21.4	AR = 8 → 14
		19.6	t/c = 0.08 → 0.14
		6.7	$\Lambda_{c/4} = 10^\circ \rightarrow 30^\circ$
Minimum TOGW A/P	TOGW:	10.4	AR = 8 → 14
		9.8	t/c = 0.08 → 0.14
		9.6	$\Lambda_{c/4} = 10^\circ \rightarrow 30^\circ$
Maximum $\frac{M PL}{TOGW}$ A/P	$\frac{M PL}{TOGW}$	-5.2	AR = 8 → 14
		-15.7	t/c = 0.08 → 0.14
		Not significant	$\Lambda_{c/4} = 10^\circ \rightarrow 30^\circ$

10 deg minimizes gross weight and fuel consumption, and is close to the maximum productivity condition. The wing sweep can be increased to 20 deg and the aspect ratio can be reduced to 12 without significantly affecting fuel consumption, gross weight, or productivity. This results in an increase in cruise speed (Mach 0.78 instead of Mach 0.76). Additionally, the wing span is reduced, which is structurally desirable to help reduce wing tip deflections.

Consequently, the near-optimum planform selected for the reference cantilever airplane has the following characteristics:

- Aspect ratio = 12
- Quarter chord sweep = 20°
- Thickness/chord ratio = 0.14/0.08 (inboard/outboard)
- Cruise Mach number = 0.78

This is the planform for Model 767-768a.

# *Contrails*

## SECTION VI

### LARGE-SPAN WING STRUCTURAL ANALYSES

The long range and large payload requirements of the design mission have resulted in study configurations with very large wing spans. Consequently, preliminary weight evaluations based on statistical methods required considerable extrapolation beyond the weight analysis data base. Detailed structural analyses were therefore made to provide analytical wing weights, and also an understanding of the elastic characteristics of the very large-span wings.

Structural analyses were made of the base cantilever wing with three different thickness/chord ratios. The base strut-braced wing was also analyzed.

The structural criteria, analysis methods, and results of the analytical structural and weight analyses are described in this section.

#### 1. STRUCTURAL SIZING CRITERIA

The structural material technology level assumed for the study (1985 technology) corresponds to in-service in the mid-1990 time period. The basic structural material was 350° cure T300 graphite/epoxy. The study wings incorporated a two-spar concept with honeycomb sandwich surfaces.

The effects of active controls have been estimated and included in the wing load calculations. Gust load alleviation was estimated to produce a 15% reduction in the incremental gust load factor, and was simulated by an appropriate reduction in dynamic gust factor. Maneuver load alleviation was approximated using selected control surface deflections.

The structural calculations did not include flutter evaluations. Although large deflections were anticipated, the wings were strength sized and the wing deflections were noted for comparative evaluations. A 2.5g limit maneuver condition and a 1.67g limit taxi condition were used.

Structural analyses ground rules are summarized in Figure 31. The structural analyses for the cantilever wing included the basic thickness/chord distribution (0.14/0.08—inboard/outboard) and two additional thickness distributions, (0.15/0.10 and 0.16/0.12). The cantilever wing thickness distributions are shown in Figure 31 along with the strut-braced wing thickness distribution. Typical structural design speeds are also shown in Figure 31.

#### 2. STRUCTURAL AND WEIGHT ANALYSES METHODS

Material requirements for the cantilever wings were determined using a computerized wing structural synthesis program, ORACLE. ORACLE combines an aerodynamic loads analysis, a simplified box-beam stress analysis, and a weight analysis of the wing box. A flow chart

- 1985 TECHNOLOGY — — — 1990 + INSERVICE
- 2-SPAR CONCEPT WITH HONEYCOMB SANDWICH SURFACES
- BASIC STRUCTURAL MATERIAL IS 350° CURE T300 GRAPHITE/EPOXY
- DESIGN CONDITIONS INCLUDE 2.5 g LIMIT MANEUVER CONDITION, 1.67 g LIMIT TAXI CONDITION, AND GUST CONDITIONS
- WINGS SIZED BY STRENGTH, NO FLUTTER SIZING, NO DEFLECTION CONSTRAINTS

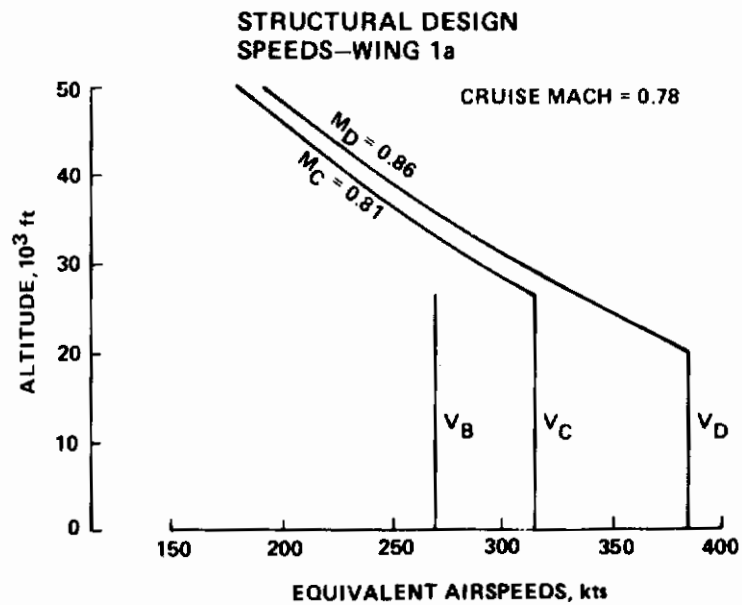
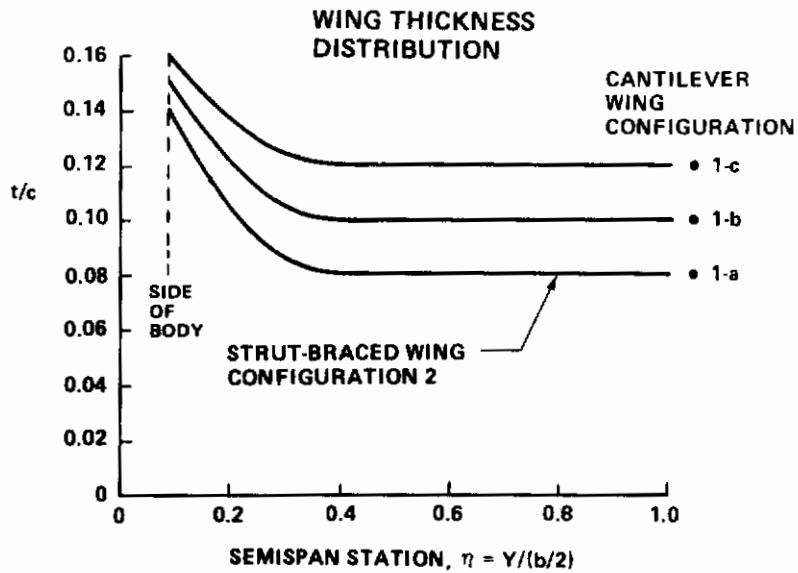


Figure 31 Structural Analysis Ground Rules

for ORACLE is shown in Figure 32. The aeroelastic loads analysis is based on beam theory and lifting line aerodynamics<sup>(5)</sup>. The elastic properties of the wings were described by bending stiffness,  $EI$ , and torsional stiffness,  $GJ$ . The box-beam stress analysis includes the effect of combined shear and axial stress.

The effects of maneuver load alleviation were investigated by deflecting either an outboard aileron with the trailing edge up, or an inboard flap with the trailing edge down.

Statistical weight estimates were used to support the initial airplane sizing exercises and the cantilever wing parametric optimization studies. These weight estimates established trends that allowed selection of desired wing planform characteristics and wing size. The statistical weight estimates required considerable extrapolation of the data base to account for the

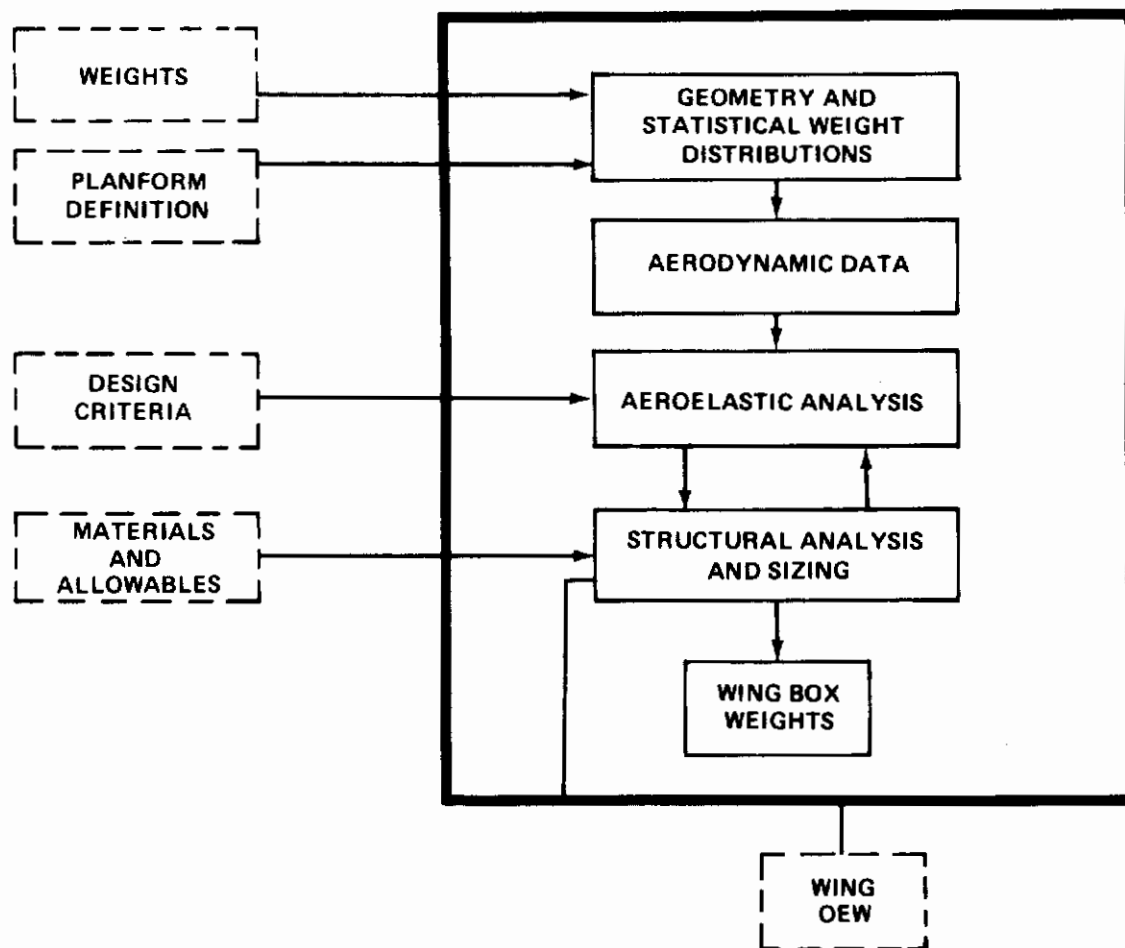


Figure 32 ORACLE—Structural Synthesis Program

5. Gray, W. L., and Schenk, K. M.: "A Method for Calculating the Subsonic Steady-State Loading on an Airplane with a Wing of Arbitrary Planform and Stiffness," NACA TN-3030, December 1953.



large size of the study airplanes and for the advanced technology. The required degree of extrapolation was minimized by scaling from analytical wing weights derived in Boeing in-house large freighter studies.

The structural analyses described in this section provided definition of the wing material requirements necessary for the analytical weight evaluations of the cantilever and strut-braced wing planforms. These theoretical evaluations of the wing primary structure, plus statistical evaluations of the secondary structural weight items, comprise the analytical weight evaluations of the large span wings. The weight analysis procedure is described in more detail in Reference 6.

Results of the structural and weight analyses of the cantilever and strut-braced wings are summarized in the sections that follow.

### 3. CANTILEVER WING STRUCTURAL ANALYSES

The locations of spars and the load reference axis used for all of the cantilever wings are shown in the planview in Figure 33. The outboard aileron and inboard flap control surfaces used in the maneuver load alleviation studies are also shown. The aileron is located between the outboard nacelle and the wing tip, and has a chord length equal to 20% of the wing chord. The inboard flap is located between the inboard nacelle and the side of the body, and has a chord length equal to 10% of the wing chord. The flap used for load alleviation is the aft part of the main flap, and was assumed to rotate about a hinge located at 90% wing chord to allow rapid action.

All of the wings were sized by a 2.5g maneuver condition and the 1.67g taxi condition. Figure 33 contains the design loads for the thinnest wing. The differences in wing thickness distributions of the three study wings (Figure 31) had little effect on the design loads.

The required equivalent structural material thicknesses of the wing boxes of the three cantilever wings are shown in Figure 34. The equivalent structural material thickness requirements decrease as the wing overall thickness/chord ratio increases. Bending and torsional stiffnesses are shown in Figure 35. Wing stiffness increases as the wing is thickened.

Vertical deflections of the cantilever wings and the strut-braced wing are shown in Figure 36 at taxi, cruise, and maneuver conditions. These results indicate an area of concern in the taxi condition, where the tip and/or outboard nacelle strike the ground. Increased wing thickness alleviates but does not cure this problem. Additional design modifications and studies would be necessary to define the most desirable solution. The strut-braced wing discussed in the next section provides a solution for wing deflection concerns during taxi, as shown in Figure 36.

6. Anderson, R. L., and Giridharadas, B.: "Wing Aeroelastic Structural Analysis Applied to the Study of Fuel-Conserving CTOL Transports," SAWE Paper No. 1040, May 1975.



MODEL 767-768

$t/c = 0.14/0.08$

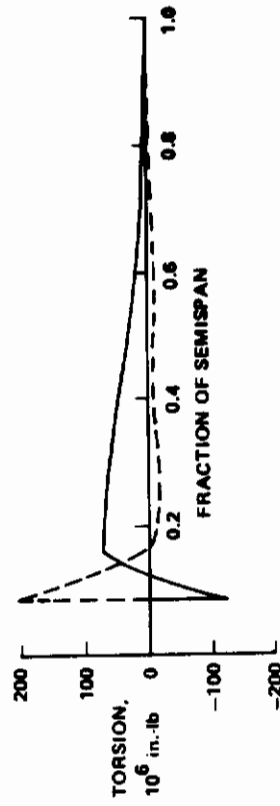
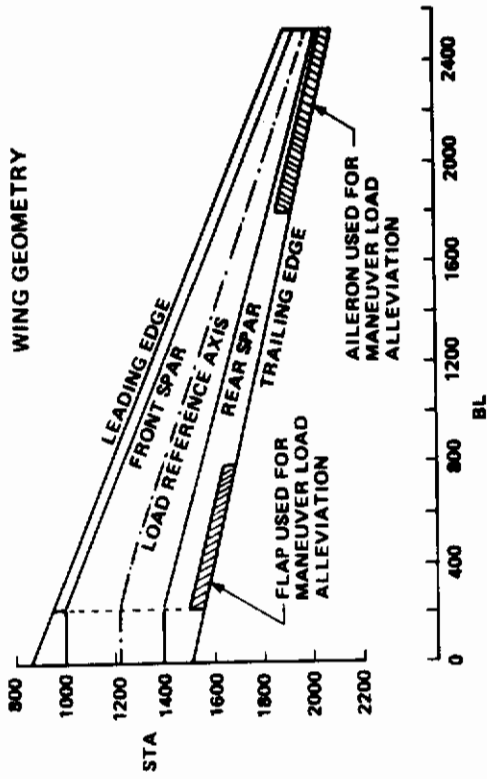
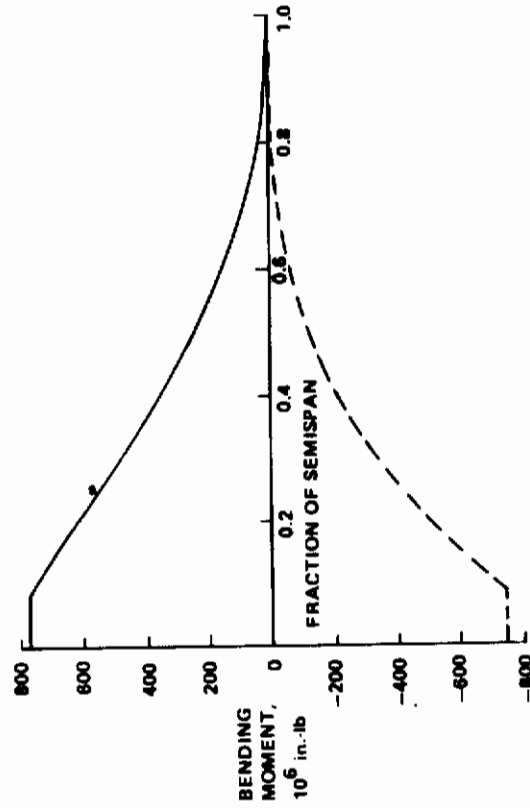
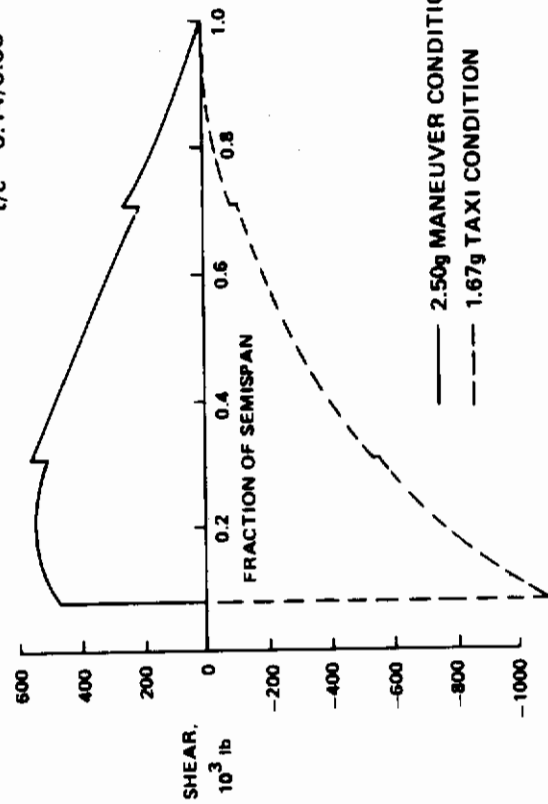


Figure 33 Cantilever Wing Structural Analyses

# Contrails

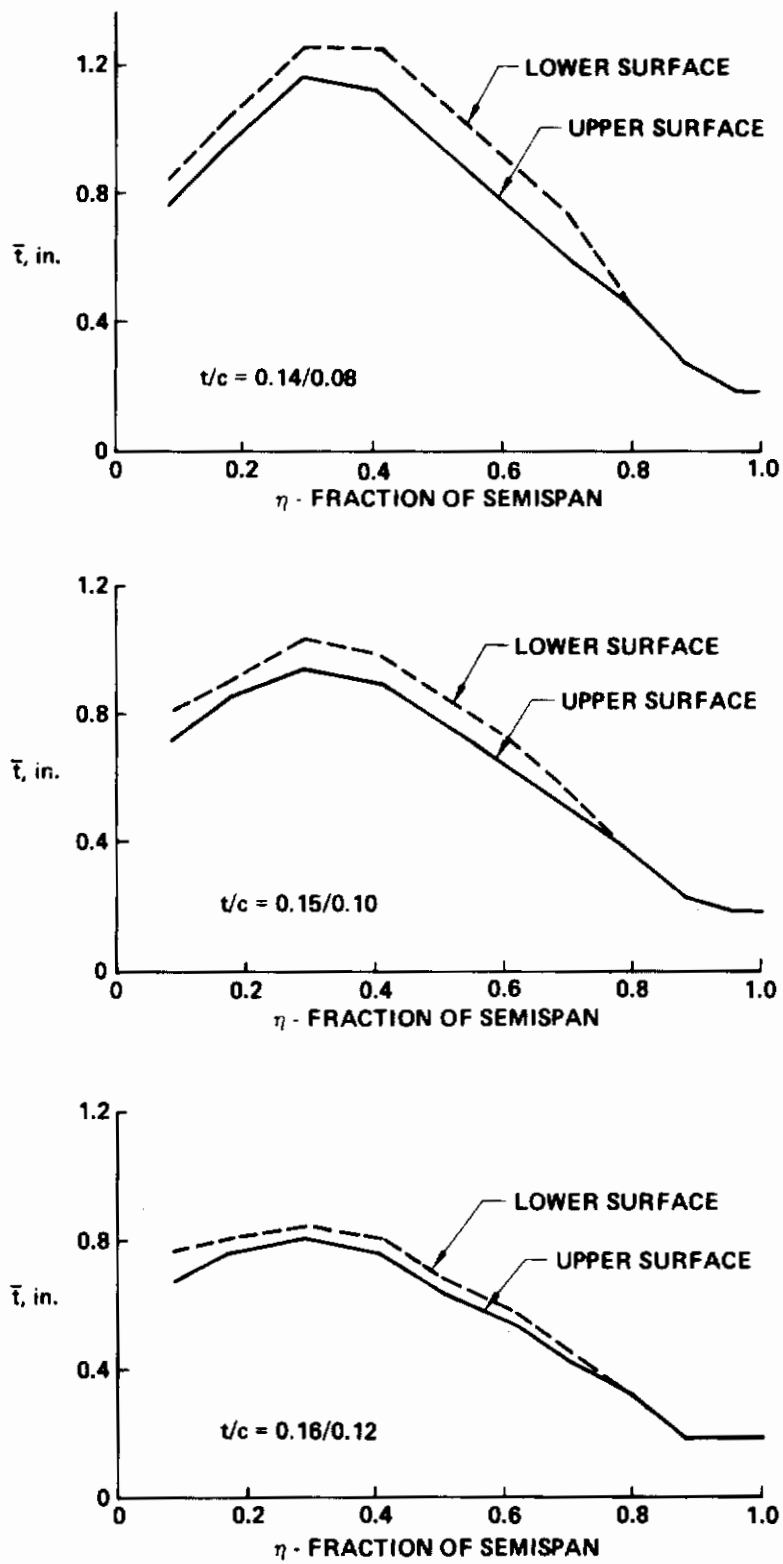


Figure 34 Cantilever Wing Equivalent Structural Material Thickness

## GRAPHITE/EPOXY SANDWICH STRUCTURE

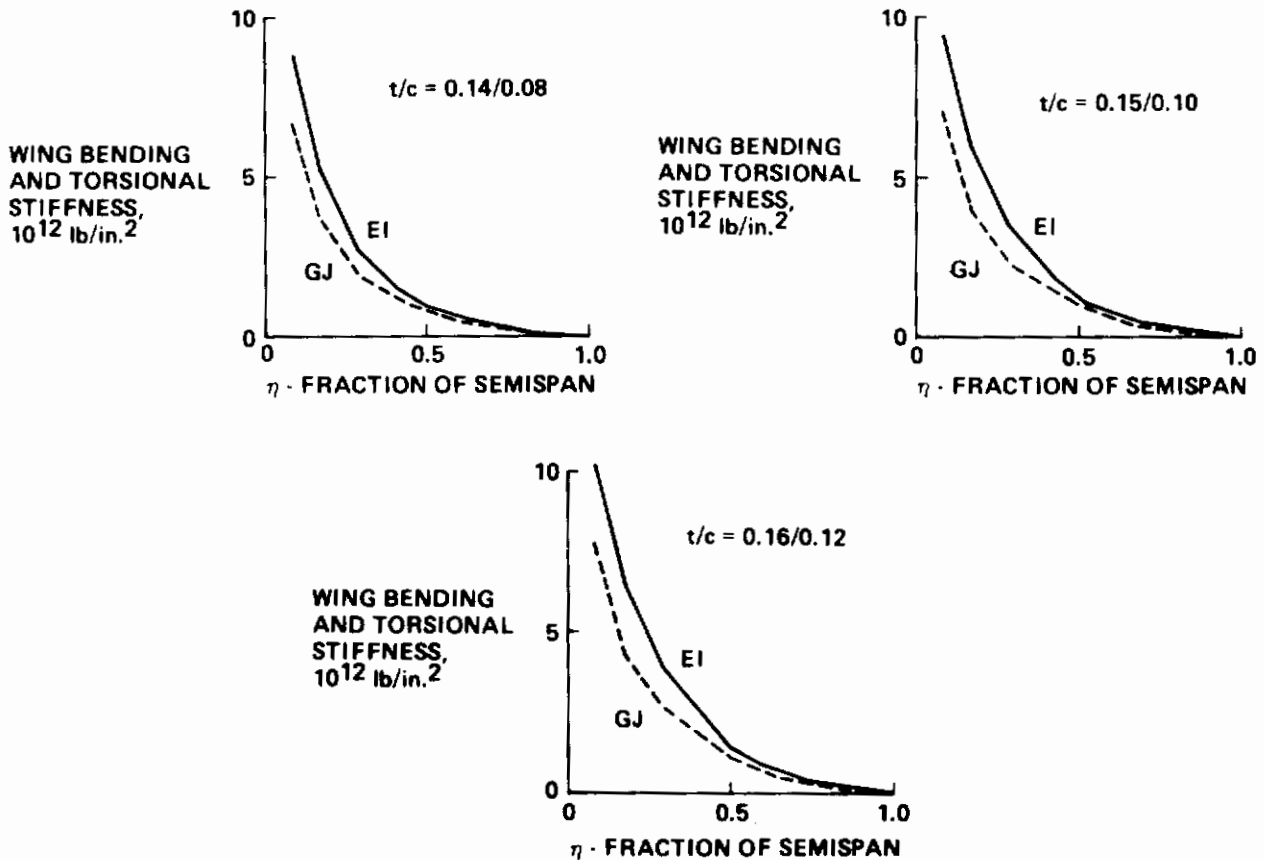


Figure 35 Cantilever Wing Stiffnesses

The effects of maneuver load alleviation (MLA) were investigated by deflecting either an outboard aileron with the trailing edge up, or an inboard flap with the trailing edge down, to try to shift wing lift loading inboard and thereby reduce the wing root bending moment. The spanwise lift distributions with and without MLA are shown in Figure 37. When the ailerons were deflected, the flexible wings tended to wash in at the tips, thereby shifting the wing lift outboard. Hence, use of the ailerons actually produced an undesirable increase in root bending moment.

When the inboard flaps were deflected, the lift loading shifted inboard, producing a desired reduction in root bending moment (Figure 37). Hence, an MLA system using the inboard flaps provided a wing weight saving for the study configurations.

Results of the wing weight evaluations based on the aforementioned structural analyses are shown in Figure 38 as weights relative to the statistical weight evaluations of the reference cantilever wing ( $t/c = 0.14/0.08$ ).

WING	AR	$\Lambda_c/A$
CANTILEVER	12	20°
STRUT-BRACED	13.4	

SYMBOL	CONDITION	LIMIT $n$
---	TAXI	1.67
---	AVERAGE CRUISE	1.0
---	MANEUVER	2.5

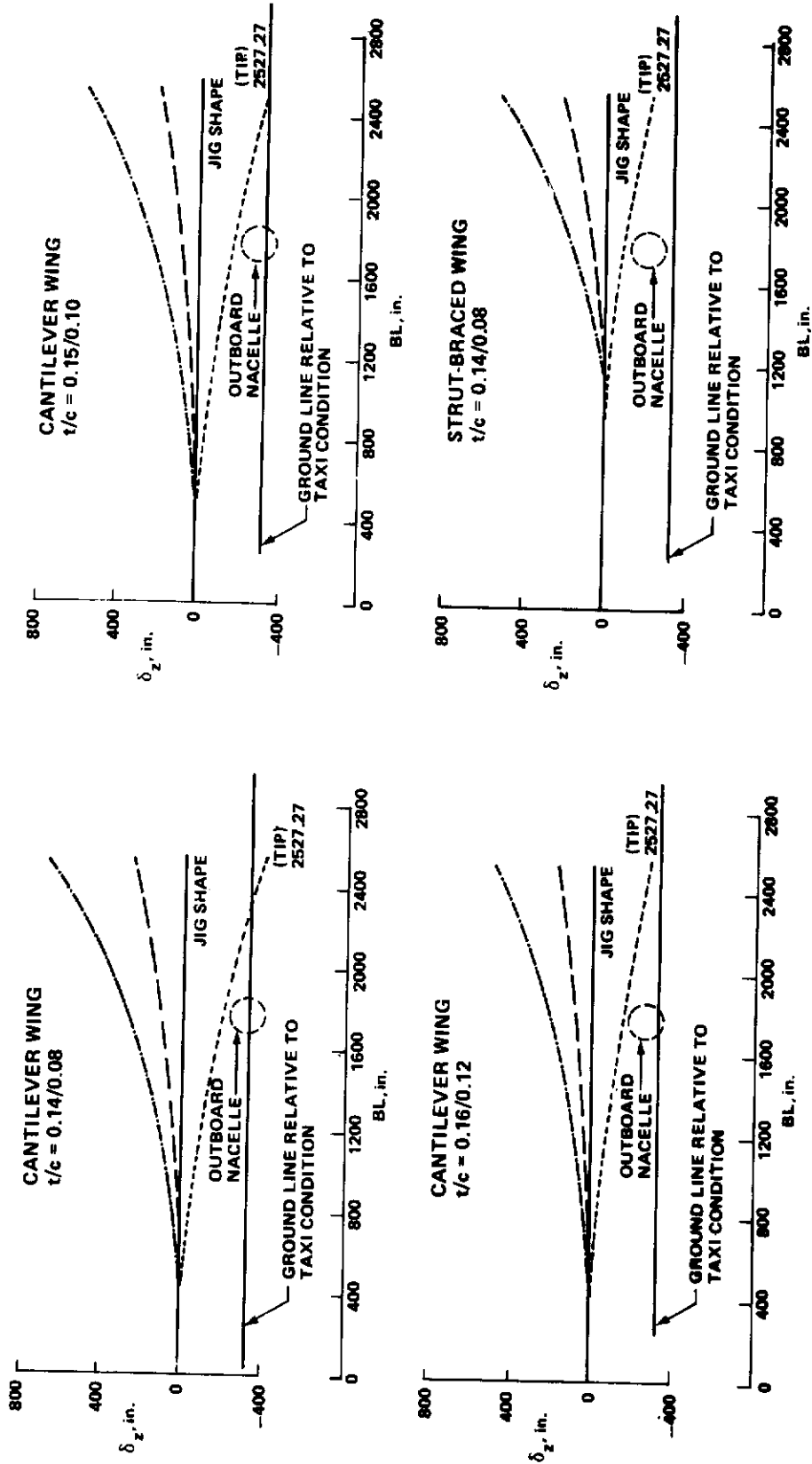


Figure 36 Large-Span Wing Deflections

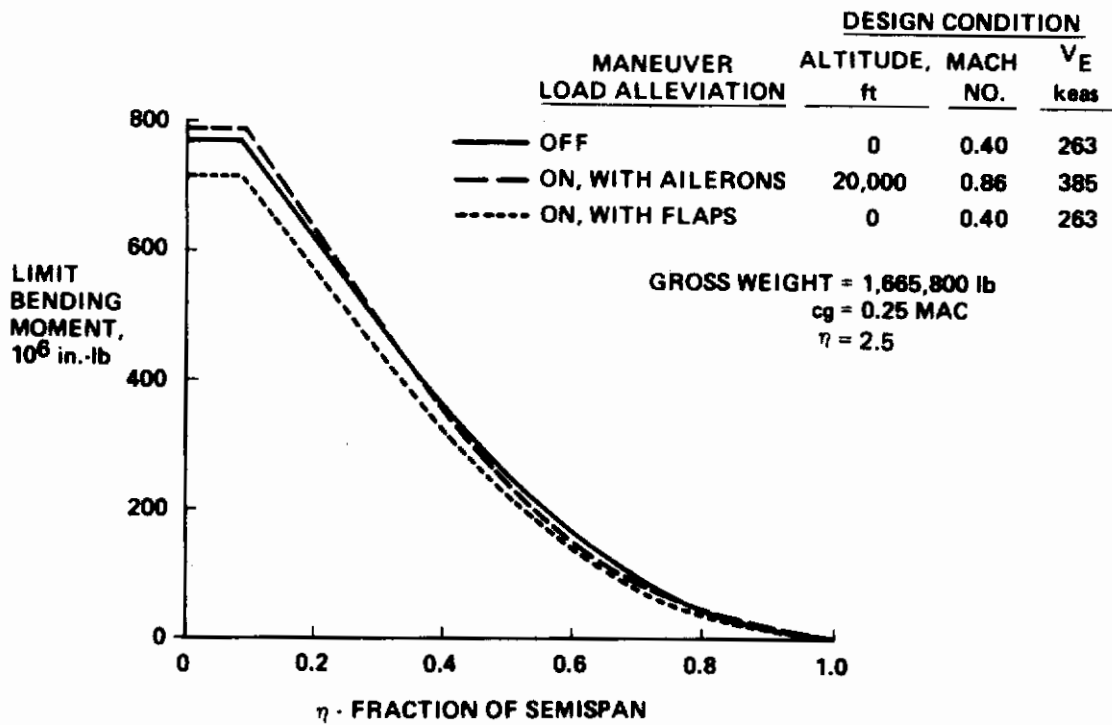
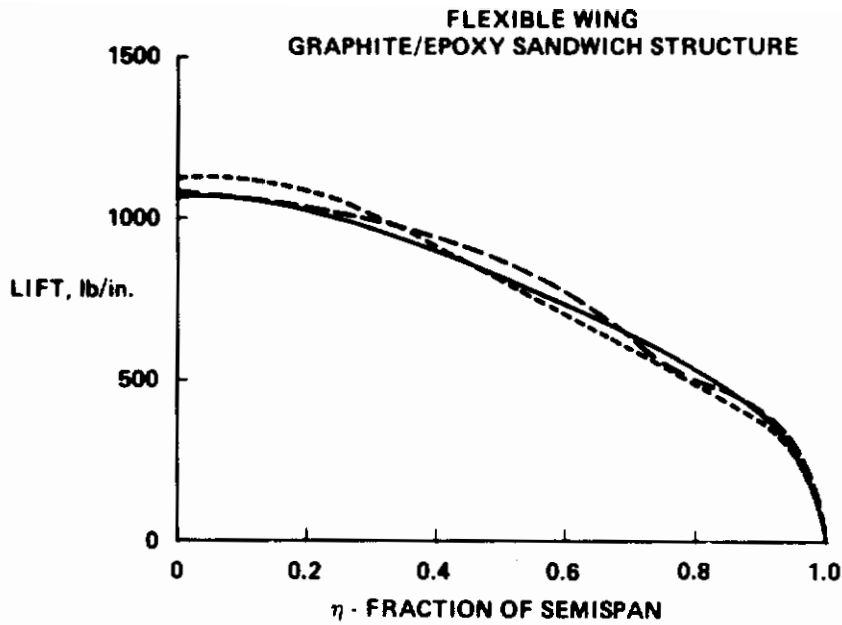


Figure 37 Wing Lift Distributions and Root Bending Moments

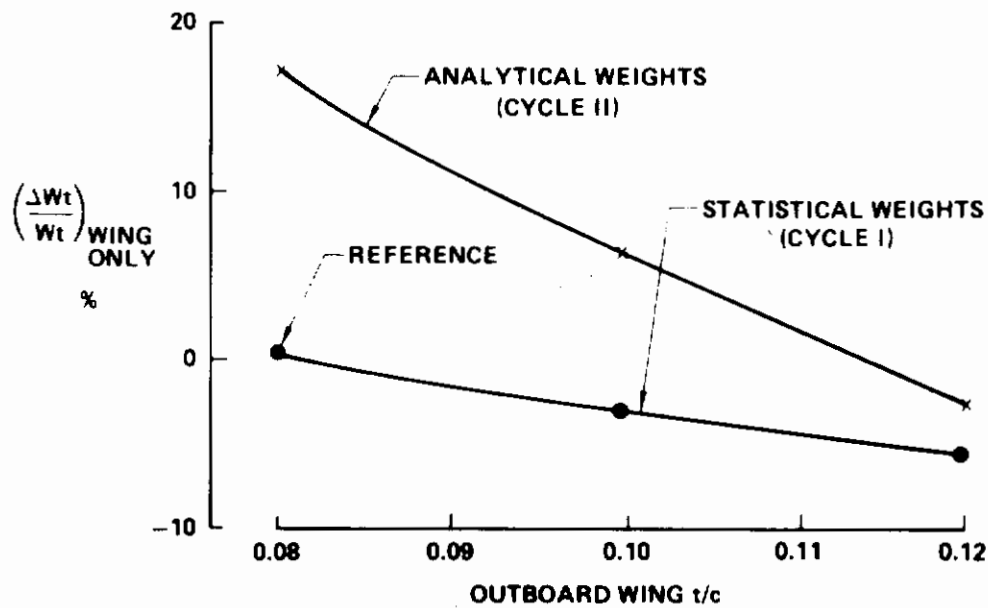


Figure 38 Comparison of Statistical and Analytical Weight Estimates—Cantilever Wings

The statistical weight analyses under-predicted the wing weights, particularly for the thinner wings. The effects of wing thickness on wing weight as predicted by the analytical and the statistical methods are similar. The impact of the differences in estimated wing weights on the fuel consumption, empty weight, and gross weight of the study airplanes is discussed in Section IV.

#### 4. STRUT-BRACED WING STRUCTURAL ANALYSES

The strut-braced wing has been structurally analyzed by the following iterative procedure. Initially, an equivalent stiffness was assumed for the portion of the wing supported by the main strut/jury strut arrangement. The beam analysis program, ORACLE, was then used to calculate the aeroelastic loads and deflections of the “equivalent” cantilever wing representation of the strut-braced wing.

The initial aeroelastic loads were then imposed on a finite element model of the wing and strut geometry with estimated stiffnesses. The finite element model provided the distribution of the loads between the strut and the wing, and the corresponding internal loads. The inboard wing and strut were resized, based on the internal loads from the finite element program, and new stiffnesses were incorporated into the modeling of the wing. Iteration was concluded when the wing and strut loads, deflections, and stiffnesses sufficiently converged. This iteration procedure is shown in Figure 39.

Initial analyses of the strut-braced wing indicated the need for a jury strut to provide a more structurally efficient wing/strut arrangement. Consequently, a jury strut was incorporated into the definition of the baseline braced wing arrangement (Figure 6).

# Contrails

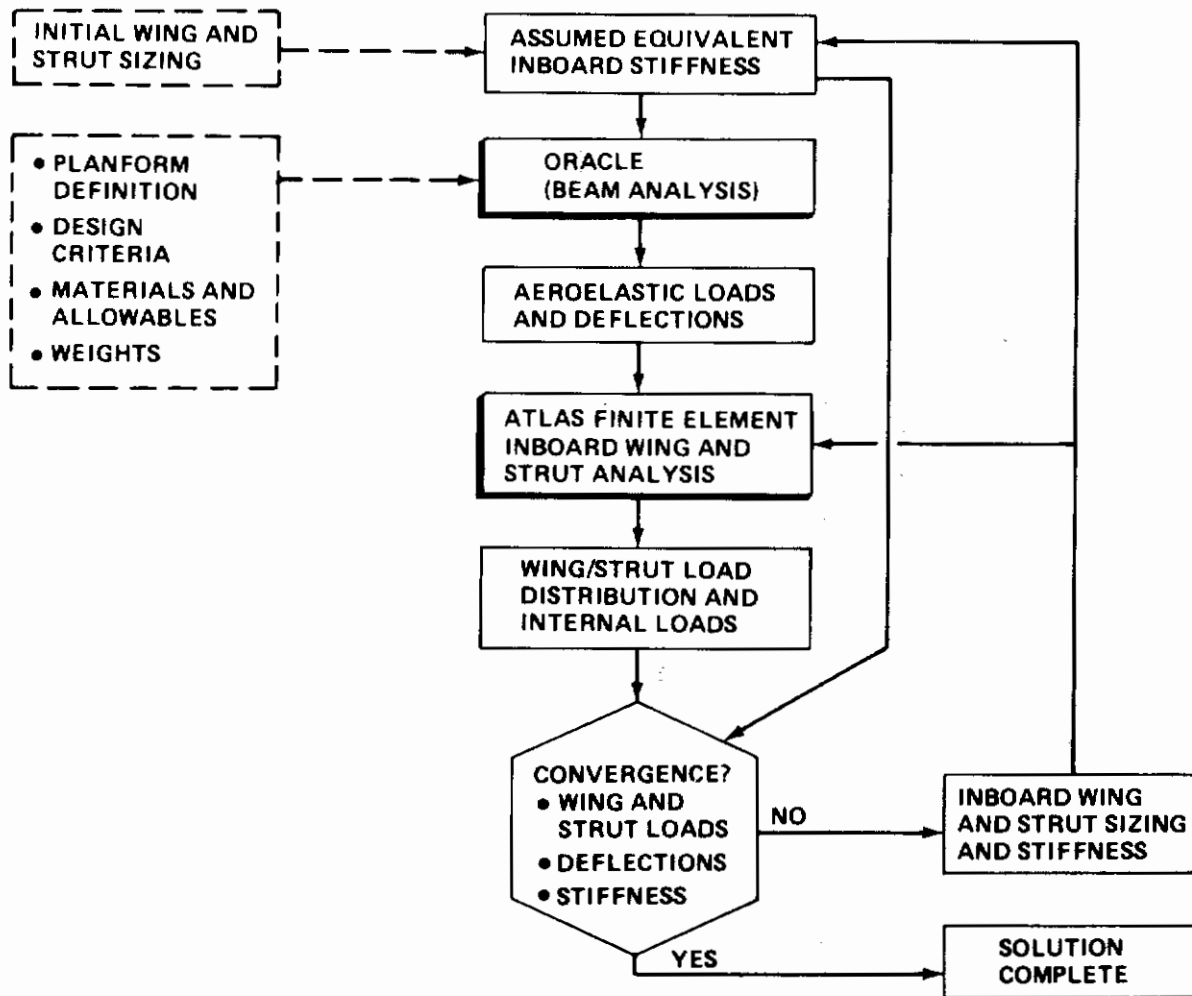


Figure 39 Strut-Braced Wing Structural Analysis Methods

The strut-braced wing spar locations are shown in Figure 40. This figure also contains the design loads for the strut-braced wing.

The required equivalent structural material thickness of the strut-braced wing is shown in Figure 41. The analytical weight of the strut-braced wing was approximately 5% higher than the statistical weight prediction.

Vertical deflections of the strut-braced wing are shown in Figure 36. The strut-braced wing concept eliminated taxi deflection concerns of the large-span wings of the study configurations.

MODEL 767-790  
 $t/c = 0.14/0.08$

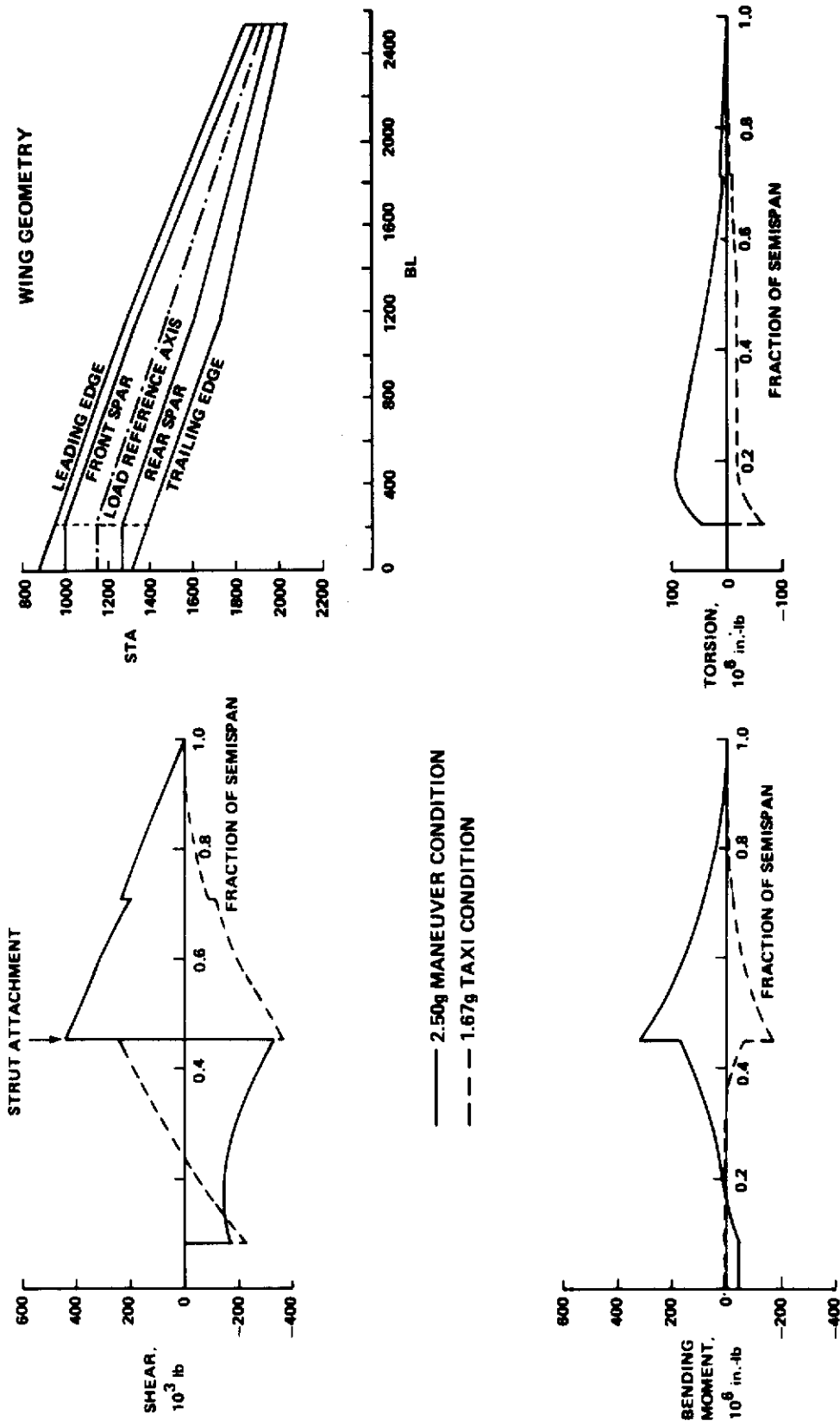


Figure 40 Strut-Braced Wing Structural Analyses



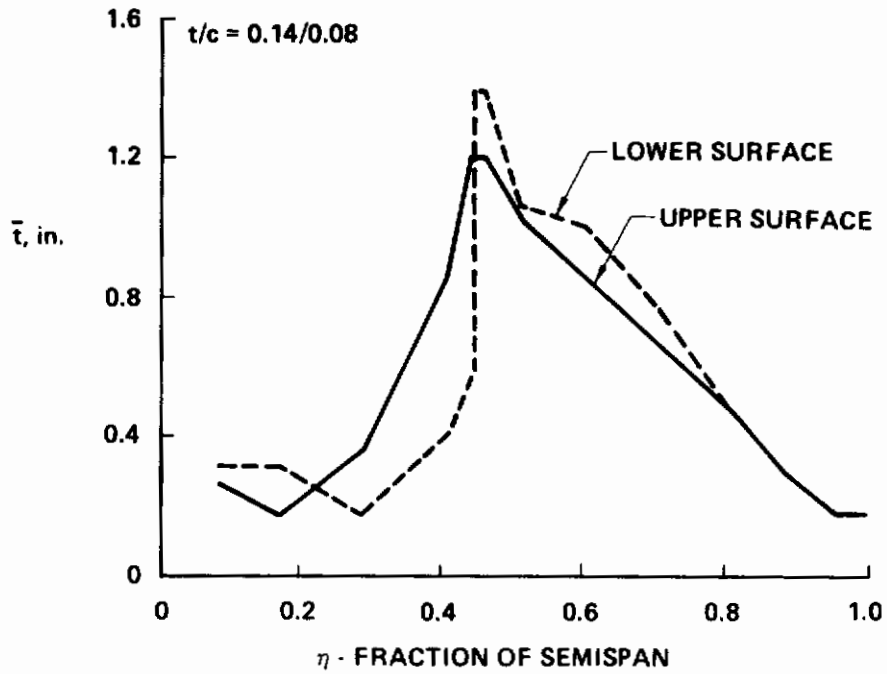


Figure 41 Strut-Braced Wing Equivalent Structural Material Thickness

# *Contrails*

## SECTION VII

### RECOMMENDATIONS

Transport aircraft configurations designed to carry large payloads over very long ranges favor relatively thin, high aspect ratio wing planforms for low gross weight and minimum fuel requirements. These very large-span wings experience large aeroelastic deflections. The large structural deflections could ultimately limit wing span lengths. Span length limits could impose a strong indirect relationship between the design mission requirements and the optimum wing planform characteristics.

The strut-braced wing concept offers a potentially structurally efficient approach to develop large-span wing designs. However, a significant number of design variables related to integrated wing/body/strut design must be investigated to arrive at an optimized design. Detailed aerodynamic design, structural design, and wind tunnel test verification studies are necessary to fully identify the potential of transport aircraft configurations employing large-span strut-braced wings.

Recommended studies necessary to determine limitations, and performance and economic benefits of very large-span transport aircraft include:

- Detailed structural design and analyses studies (including flutter) with aluminum structure, and also with advanced composites materials, to identify design limitations and performance potential of very large-span cantilever wings.
- Aerodynamic design studies and wind tunnel test verification studies to minimize wing/strut interference effects on profile and compressibility drag. The use of emerging advanced aerodynamic design and analysis methods capable of properly modeling the wing/strut intersection, including viscosity effects and three-dimensional transonic flow, would be very desirable.
- Detailed design and structural analyses (including flutter) of strut-braced wings with aluminum structure, and also with advanced composites materials, to define design limitations and weight characteristics of large span-braced wings.
- Parametric detailed design studies to determine optimum wing/strut geometry characteristics.
- Range/payload studies to explore the impact of design objectives and criteria on optimum wing/strut characteristics and on structural design limitations.

# *Contrails*

## SECTION VIII

### CONCLUSIONS

The purpose of the study was to conduct a preliminary design investigation of very large, long-range turbulent flow military transport aircraft. Performance and economic comparisons were made between strut-braced wing and cantilever wing configurations.

Major conclusions of the study that apply specifically to very long-range, high-payload military transport airplanes of relatively low utilization are:

- Based on parametric statistical weights, the best cantilever wing planform for minimum takeoff gross weight (TOGW), and minimum fuel requirements has a high aspect ratio, low sweep, low thickness/chord ratio, and a cruise Mach number of 0.76.
- A near optimum planform with greater speed capability has:
  - Aspect ratio = 12
  - Quarter chord sweep = 20 deg
  - Thickness/chord ratio = 0.14/0.08, (inboard/outboard)
  - Cruise Mach = 0.78
- Results obtained with the more accurate analytic weights confirmed the parametric statistical weights result: that the thinnest wing ( $t/c = 0.14/0.08$ ) is the best for minimum fuel. However, the analytic weight results indicated that minimum TOGW is achieved by increasing the wing thickness ratio to  $t/c = 0.15/0.10$ . The cruise speed would be reduced to  $M = 0.76$ . The minimum empty weight occurred with the wing thickness ratio further increased to  $t/c = 0.16/0.12$ . The cruise Mach number in this case would be reduced to 0.74.
- Results of the structural analyses indicated that the very large-span cantilever wing designs experience significant deflections. Increasing the wing thickness tended to alleviate taxi condition deflection concerns at the expense of increased fuel requirements.
- Additional detailed design and structural analyses are necessary to establish design limitations of very large-span cantilever wings.
- Based on analytic (structural analyses) weights and projected improvements in wing/strut aerodynamic designs, the strut-braced wing offers the potential of lower gross weight, lower empty weight, and reduced fuel consumption.
- The strut-braced wing design was effective in reducing taxi deflections of very large-span wings.

# *Contrails*

- Aerodynamic design and wind tunnel test verification studies are necessary to fully identify the wing/strut integration aerodynamic effects.
- Additional wing/strut design investigations and structural analyses are necessary to optimize the design of a very large-span strut-braced wing.

## REFERENCES

1. Kulfan, R. M., and Howard, W. M.: "Application of Advanced Aerodynamic Concepts to Large Subsonic Transport Airplanes," Tech. Report AFFDL-TR-75-112, November 1975.
2. Kulfan, R. M., and Vachal, J. D.: "Application of Laminar Flow Control to Large Subsonic Military Transport Airplanes," Tech. Report AFFDL-TR-77-65, July 1977.
3. Wallace, R. E.: "Parametric and Optimization Techniques for Airplane Design Synthesis," Paper No. 7 in AGARD-LS-56, April 1972.
4. Healy, M. J.; Kowalik, J. S.; and Ramsay, J. W.: "Airplane Engine Selection by Optimization on Surface Fit Approximations," Journal of Aircraft, Vol. 12, No. 7, July 1975.
5. Gray, W. L., and Schenk, K. M.: "A Method for Calculating the Subsonic Steady-State Loading on an Airplane with a Wing of Arbitrary Planform and Stiffness," NACA TN-3030, December 1953.
6. Anderson, R. L., and Giridharadas, B.: "Wing Aeroelastic Structural Analysis Applied to the Study of Fuel-Conserving CTOL Transports," SAWE Paper No. 1040, May 1975.